

This is the **accepted version** of the journal article:

Faggi, Enrico; Gascó-Catalán, Carolina; Aguilera-Sigalat, Jordi (CUANTUM Medical Cosmetics S.L.); [et al.]. «Polymethylferrocene-induced photopolymerization of cyanoacrylates using visible and near-infrared light». *Macromolecules*, Vol. 52, Issue 15 (August 2019), p. 5602-5610. DOI 10.1021/acs.macromol.9b00745

This version is available at <https://ddd.uab.cat/record/266061>

under the terms of the  ^{IN} COPYRIGHT license

Polymethylferrocene-induced photopolymerization of cyanoacrylates using visible and near-infrared light

Enrico Faggi,^a Carolina Gascó,^a Jordi Aguilera,^b Gonzalo Guirado,^a Sara Ortego,^b Rubén Sáez,^b Ferran Pujol,^b Jordi Marquet,^a Jordi Hernando,^{a,} and Rosa María Sebastián^{a,*}*

^a Departament de Química, Universitat Autònoma de Barcelona, Cerdanyola del Vallès, Spain

^b CUANTUM Medical Cosmetics S.L., Cerdanyola del Vallès, Spain

KEYWORDS: cyanoacrylates, photopolymerization, photoinduced electron transfer, polymethylferrocenes

ABSTRACT

Metallocene-induced photopolymerization of cyanoacrylates based on electron transfer processes has been proposed as an alternative to more conventional light-curing strategies relying on photobase generators. However, successful application of this methodology has so far only been achieved for very reactive cyanoacrylates under UV illumination and long irradiation times,

which eventually hampers its practical use. To overcome these limitations, we describe in this work the use of electron-rich polymethylferrocenes as photoinitiators, with which fast light-induced polymerization of commercial formulations of less reactive, but more relevant long alkyl chain cyanoacrylates has been accomplished by illumination with visible and even near-infrared light. In addition, generalization of this technology to other electron-deficient, non-cyanoacrylate monomers has been demonstrated. The low oxidation potential of polymethylferrocenes accounts for these excellent results, which strongly favors the formation of radical anions by electron transfer that initiate the polymerization reaction. Because of the high molecular weight and superior adhesive behavior of the resulting polymer materials as well as the facile access to polymethylferrocenes, they emerge as very attractive photoinitiators for the light-curing of cyanoacrylate (and other) glues in real applications.

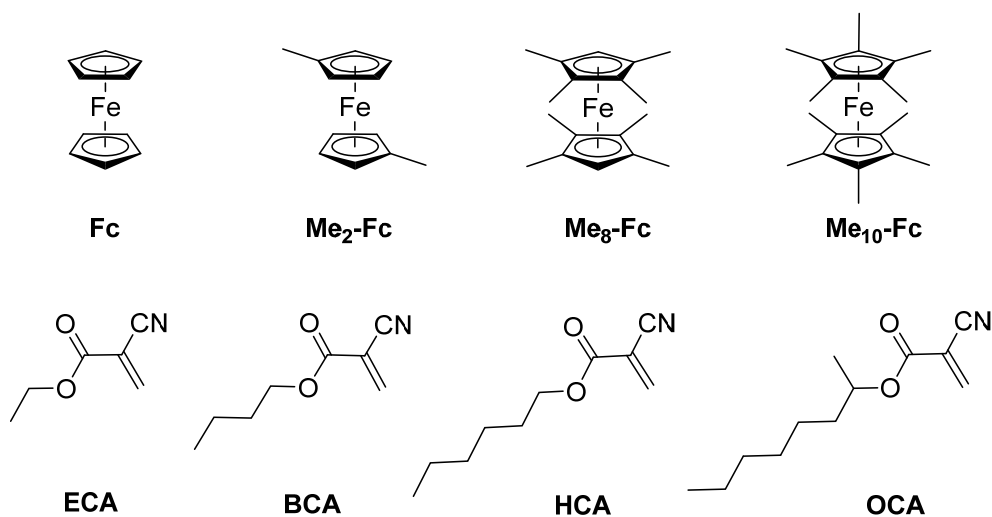
INTRODUCTION

Photopolymerization has become a very popular strategy in macromolecular synthesis¹⁻⁴ that is currently exploited in a number of practical applications (e.g. dental fillings,⁵ 3D printing^{6,7} and adhesives⁸). Among the different types of photochemical reactions employed in this area, photoinduced electron transfer (PET) processes are gaining increasing importance due to their capacity to not only initiate polymerization processes, but also to accurately control the molecular weight, monomer sequence and structure of the final macromolecules.⁹ As a result, PET has been profusely explored to conduct radical, cationic and even step-growth polymerizations; however, their use in anionic polymerization reactions has been so far very scarce.⁹

One of the few examples described of PET-induced anionic polymerization is the light-curing of cyanoacrylates (CA), well-known adhesives for the industrial and consumer markets¹⁰⁻¹² that are finding application in other emerging areas (e.g. in the medical, veterinary and cosmetic fields¹³⁻¹⁵). When irradiating cyanoacrylate solutions of ferrocene or ruthenocene, electrons are transferred from the metallocenes to the surrounding monomers, which generates CA^{•-} radical anions that are capable of initiating the polymerization process,^{16,17} as supported by computational calculations.¹⁸ Because of the simplicity of this mechanism and the low thermal reactivity, cost and toxicity of ferrocene,¹⁹ this methodology would be an excellent alternative to more traditional cyanoacrylate photopolymerization strategies relying on photobase generators,²⁰⁻²⁸ which require the use of organometallic complexes of low biocompatibility metals (e.g. chromium, platinum or tungsten),²⁰⁻²² poorly stable photoinitiator-monomer mixtures,²⁷ and/or the previous synthesis of photoinitiators.^{21,25-28} Unfortunately, ferrocene-induced photopolymerization of cyanoacrylates has only shown to work for short alkyl chain, very reactive monomers under UV illumination and relatively long irradiation times,¹⁶ thus severely compromising its practical use. For this methodology to have a true impact on light-controlled CA-based adhesives curing (e.g. for biomedical applications¹³⁻¹⁵), it should allow for short adhesion setting times under visible light irradiation when applied to long alkyl chain, less reactive monomers with superior properties. This is the case of butyl 2-cyanoacrylate and 2-octyl 2-cyanoacrylate, which possess lower toxicity, higher viscosity, and larger stability and flexibility upon curing.^{10-11,13}

To reach these objectives we investigated herein the use of polymethylferrocenes, electron-rich ferrocene derivatives that should be more prone to undergo PET processes with cyanoacrylates under irradiation and, as such, favor CA^{•-} formation and subsequent polymerization. In particular,

we considered the use of three different ferrocene-based photoinitiators (1,1'-dimethylferrocene, **Me₂-Fc**; octamethylferrocene, **Me₈-Fc**; decamethylferrocene, **Me₁₀-Fc**), which together with pristine ferrocene (**Fc**) were applied to the light-induced curing of a diversity of CAs: highly reactive ethyl 2-cyanoacrylate (**ECA**) and less reactive butyl 2-cyanoacrylate (**BCA**), hexyl 2-cyanoacrylate (**HCA**) and 2-octyl 2-cyanoacrylate (**OCA**, Scheme 1). Detailed mechanistic studies were conducted to rationalize the light-induced reactivity observed for the resulting photoinitiator-monomer mixtures and, in an attempt to broaden the scope of this methodology, its application to other, non-cyanoacrylate systems was also explored.



Scheme 1. Metallocenes and reactive monomers investigated in this work to accomplish PET-induced polymerization of cyanoacrylates.

EXPERIMENTAL SECTION

Materials and general methods. Reagents and solvents for the synthesis of **Me₈-Fc** and photoinitiators **Fc**, **Me₂-Fc** and **Me₁₀-Fc** were purchased and used without further purification.

When required, solvents were dried using standard procedures. Reactions requiring an inert atmosphere were conducted under nitrogen or argon using standard Schlenk techniques. Reactive monomers **ECA**, **BCA**, **HCA**, **OCA** and diethyl methylenemalonate were provided by Cuantum Medical Cosmetics S.L. and employed as received, whereas tetrahydrofurfuryl acrylate was acquired commercially and passed through a short silica pad to remove the excess of radical stabilizer before use. NMR spectra were recorded using a Bruker spectrometer DXP360 (360 MHz (^1H); 90 MHz (^{13}C), respectively). ^1H and ^{13}C chemical shifts are reported in ppm relative to tetramethylsilane, using residual proton and ^{13}C resonances from solvent as internal standards. Infrared spectra were recorded using a Bruker Tensor 27 instrument equipped with an ATR Golden Gate cell and a diamond window.

Synthesis of Me₈-Fc. This compound was prepared from commercially available products according to a reported procedure²⁹ (90% yield). ^1H NMR (360 MHz, CDCl_3): δ 3.41 (s, 2H), 1.81 (s, 12H), 1.76 (s, 12H). ^{13}C NMR (90 MHz, CDCl_3): δ 80.4, 80.3, 70.8, 11.8, 9.8.

Electro-optical characterization. Steady-state UV-vis absorption measurements were recorded on a HP 8453 spectrophotometer using 1 cm-thick quartz cuvettes in acetonitrile (HPLC quality). Cyclic voltammograms were registered using a CHI600E potentiostat and a conical electrochemical cell equipped with an argon bubbling source for degassing, a glassy carbon working electrode (WE, $d = 1.02$ mm), a glassy carbon auxiliary electrode (CE, $d = 3$ mm) and a saturated calomel reference electrode (SCE). All the potentials are reported versus a SCE isolated from the working electrode by a salt bridge. Spectroelectrochemical experiments were performed in a 0.33 mm thin layer quartz glass cell using platinum gauze and platinum wire as working and counter electrodes, respectively, whereas a SCE was used as a reference electrode. A PC-controlled VSP-Potentiostat synchronized with an MMS-UV-vis high speed diode array

spectrometer with a bandwidth of 300–1100 nm and a deuterium/tungsten light source coupled to an optical fiber was employed to register the spectroelectrochemical measurements. Each spectrum was recorded after 0.05 s. BioKine32 software was used for data acquisition and treatment. Electrolysis experiments at controlled potentials were undertaken with an EG&G Princeton Applied Research (PAR) 273A potentiostat and an electrochemical cell equipped with an argon bubbling source. The cell consisted in a 25 mL cylindrical vessel made of vitreous carbon (working electrode), to which an auxiliary platinum electrode and a SCE reference electrode were added. All these electrochemical measurements were performed in dry acetonitrile solution containing 0.1 M of *n*-Bu₄NPF₆ as a supporting electrolyte. To prevent undesired thermal cyanoacrylate polymerization, all glass material used in these experiments was previously passivated with acid.

Stabilization of monomers. The batches of CA monomers and diethyl methylenemalonate received were already loaded with certain amounts of acid and radical stabilizers. To estimate the quantity of acid stabilizers in these samples that could interfere with their anionic photopolymerization reaction, a viscosity acid value determination (AVD) technique previously described³⁰ was employed. In this technique, a solution of a tertiary amine is mixed quickly with 0.5 mL of a chosen reactive monomer. The resulting mixture is manually stirred with a wooden stick until it cannot be separated from the mixture anymore, as it gets stuck in it. The time elapsed between the mixing and the sticking is defined as *t*_{AVD}. *t*_{AVD} is used to quantify the amount of acid stabilizers, which were found to be different for each type of reactive monomer (Table S1).

Photopolymerization experiments. To study the light-induced polymerization of the reactive monomers, calorimetric experiments were performed. In each of these experiments, a closed

polypropylene well (diameter: 9 mm) was filled with 100 μL of a liquid monomer where the photoinitiator of choice had been previously dissolved (typically, $0.5 \cdot 10^{-3} \text{ M}$). The sample was then irradiated with a hand-held LED ($\lambda = 420 \text{ nm}$, power = 46 mW cm^{-2} , photon flux = $1.1 \cdot 10^{-7} \text{ Einstein s}^{-1}$) or a cw diode laser ($\lambda_{\text{exc}} = 780 \text{ nm}$, power = 320 mW cm^{-2} , photon flux = $5.2 \cdot 10^{-7} \text{ Einstein s}^{-1}$) and its temperature was monitored with an infrared probe and recorded every second until minimal thermal changes were observed. In all the cases, an increase of temperature (typically, $\Delta T = 8\text{-}18 \text{ }^\circ\text{C}$) was observed as a consequence of CA polymerization, which is a strongly exothermic process. To estimate the time period needed for photopolymerization to occur, we determined the time at which the sample temperature rise was half of the overall increase observed during the calorimetric experiment (*i.e.* when $T = T_0 + 0.5 \Delta T$, t_{photo}). Because of the sigmoidal shape mostly observed for temperature variation in these experiments, t_{photo} can be assigned to the time at which the thermal change is higher and, assuming fast heat diffusion for the small sample volume, at which polymerization reaction rate reaches its maximum. Several replicates ($n = 3$) were conducted for each monomer-photoinitiator pair and reproducible t_{photo} values were retrieved. Additional calorimetric experiments were undertaken where a small Teflon stirring bar was added to the polypropylene well ($\sim 50 \text{ rpm}$), which was found to stop spinning when the sample became viscous enough as a result of photopolymerization. In all the cases, this phenomenon was observed to occur slightly before t_{photo} ($\sim 3\text{-}8 \text{ s}$), since a relatively small increase in viscosity is enough to prevent it.³¹ Finally, we also monitored the photopolymerization of **BCA** with **Me₁₀-Fc** by means of IR spectroscopy. To this end, the ATR-IR spectra of **BCA** monomer, a fully cured **BCA+Me₁₀-Fc** mixture and a **BCA+Me₁₀-Fc** mixture at t_{photo} were acquired in the same conditions. The integrals (I) of the peaks at 3128 cm^{-1} (=C-H stretching band) and 2985 cm^{-1} (-C-H stretching band) were compared. For **BCA**,

$I_{3128}/I_{2985} = 0.167$; for the fully cured **BCA+Me₁₀-Fc** mixture, $I_{3128}/I_{2985} = 0$ as the peak at 3128 cm^{-1} is not present; for a **BCA+Me₁₀-Fc** mixture at t_{photo} , $I_{3128}/I_{2985} = 0.035$. From this data we estimated that in the latter case the mixture is composed by 79% polymer and 21% monomer.

Thermal polymerization experiments. For sake of comparison with the results of the photopolymerization experiments, thermal polymerization of monomers was also conducted by simply adding 0.5 mL of each monomer between two non-passivated glass plates and storing the sample at room temperature and in the dark for the appropriate time (typically, overnight).

Characterization of polymers. The molecular weight distribution of thermally- and light-cured polymers was determined by gel permeation chromatography (GPC) using an Agilent Technologies 1260 Infinity chromatograph and THF as a solvent. The instrument is equipped with three gel columns: PLgel 5 μm Guard/50 \times 7.5 mm, PLgel 5 μm 10000 Å MW 4K–400K, and PL Mixed gel C 5 μm MW 200–3M. Calibration was made by using PMMA standards. In each experiment, the freshly-prepared polymer sample of interest was dissolved (5 mg/mL) in THF containing 0.05% methanesulfonic acid and immediately analyzed by GPC (1 mL/min flow; 30 °C column temperature). Methanesulfonic acid was added to slow down depolymerization, a well-known process that affects polycyanoacrylates even in the solid state and leads to the formation of low molecular weight "daughter" polymer chains over time.³²

Adhesion tests. The adhesion tests were carried out following the specifications of the “ISO 4587 Adhesives Tensile Lap Shear Strength Rigid to Rigid” standard method, using an Instron 3366 instrument. They were performed on poly(methyl methacrylate) rectangular cuboid (100 x 20 x 2 mm) specimens bound with 25 μL of different adhesives: neat **ECA**, **BCA** and **OCA** and $0.5 \cdot 10^{-3}$ M solutions of **Me₁₀-Fc** in **ECA**, **BCA** and **OCA**. The lap joint area was approximately

100 mm². In the case of the monomer-**Me**₁₀-**Fc** mixtures, the specimens were clamped together and the lap joint area was irradiated at 420 nm (power = 46 mW cm⁻²) during 2 minutes, and then they were left standing during 30 min or 24 h. In the case of neat cyanoacrylates, the specimens were clamped together after the application of the adhesive, and left standing during 30 min or 24 h.

RESULTS AND DISCUSSION

Electro-optical properties of ferrocene-based photoinitiators for cyanoacrylate polymerization. Although free radical initiation of cyanoacrylate polymerization has also been described,³³ it normally proceeds via an anionic (or zwitterionic) mechanism due to the presence of strong electron-withdrawing substituents in CA monomers, which make their carbon-carbon double bond very reactive with nucleophiles.^{10,11} As a result, these monomers are electron-deficient and must actuate as good electron acceptors in PET processes. To corroborate this behavior, the reduction potentials of **ECA**, **BCA**, **HCA** and **OCA** were determined from cyclic voltammetry measurements (Table 1 and Figure S1). In all the cases, a one-electron irreversible reduction wave was registered at rather low potentials, the value of which showed little variation with the length of the monomer side alkyl chain ($E_{\text{red}} \sim -1.6$ V vs SCE in acetonitrile). In view of these results, all the cyanoacrylates considered in this work could undergo photoinduced electron transfer reactions when placed in contact with good electron donors. This is the case of ferrocene,^{16,17,34} which presents a low oxidation potential ($E_{\text{ox}} \sim +0.50$ vs SCE in acetonitrile). This behavior is further enhanced in electron-rich ferrocene derivatives such as polyalkylferrocenes, the reason for which we explored the use of these compounds as electron donors for PET-induced polymerization of cyanoacrylates.

Table 1. Electro-optical properties of CA monomers and ferrocene-based photoinitiators^a

Compound	E_{red} (V vs SCE) ^b	E_{ox} (V vs SCE) ^c	$\lambda_{\text{abs,max}}$ (nm) ^d	$\epsilon_{\text{abs}}^{\lambda_{\text{max}}}$ (M ⁻¹ cm ⁻¹)
ECA	- 1.54	-	- ^e	-
BCA	- 1.65	-	- ^e	-
HCA	- 1.55	-	- ^e	-
OCA	- 1.62	-	- ^e	-
Fc	-	+ 0.50	441	99
Me₂-Fc	-	+ 0.24	438	107
Me₈-Fc	-	- 0.06	426	116
Me₁₀-Fc	-	- 0.15 ^f	424	112

^a In acetonitrile at room temperature. 0.1 M of *n*-Bu₄NPF₆ was added in the electrochemical measurements as a supporting electrolyte. ^b E_{red} corresponds to the cathodic peak potential at 0.5 V s⁻¹. ^c E_{ox} corresponds to the half-wave anodic potential at 0.5 V s⁻¹. ^d Spectral maxima of the absorption band in the visible spectrum. ^e CA monomers show no absorption in the visible spectrum (Figure S2). ^f Because of solubility issues, a 1:1 acetonitrile:toluene mixture was used as a solvent in this case.

In particular, we focused our attention on **Me₂-Fc**, **Me₈-Fc** and **Me₁₀-Fc** since they (a) are commercially available (**Me₂-Fc** and **Me₁₀-Fc**) or can be easily prepared (**Me₈-Fc**),²⁹ and (b) present different oxidation potentials, which allowed us to analyze the effect of their electron donor properties on the PET-driven curing of cyanoacrylates. Indeed, our cyclic voltammetry measurements showed that these compounds exhibit a one-electron reversible oxidation wave whose half-wave potential decreases with the number of electron-donating methyl substituents (Table 1 and Figure 1a). By contrast, smaller differences were found in their optical properties and a weak absorption band in the visible region ($\lambda_{\text{abs,max}} \sim 430$ nm) was registered for all the

metallocenes investigated in organic solution (Table 1 and Figure 1b and S3). Importantly, this could allow CA photopolymerization using these compounds to be triggered with visible light, an essential condition for potential applications in the medical and cosmetic fields.

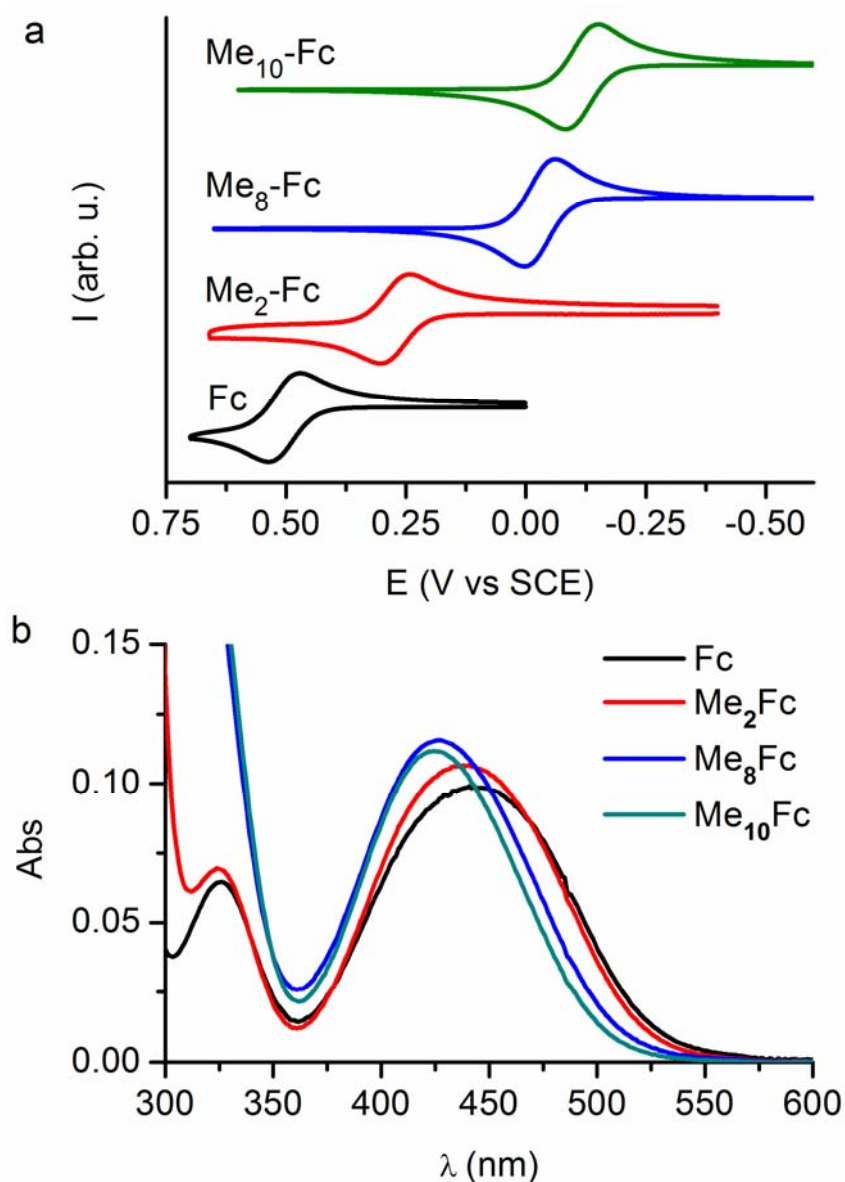


Figure 1. (a) Cyclic voltammograms of **Fc**, **Me₂-Fc**, **Me₈-Fc** and **Me₁₀-Fc** ($c \sim 3 \cdot 10^{-3}$ M) in acetonitrile (+ 0.1 M *n*-Bu₄NPF₆; scan rate = 0.5 V s⁻¹). To ensure good solubility for **Me₁₀-Fc**, a

1:1 mixture of acetonitrile and toluene was employed as a solvent in this case. (b) Absorption spectra of **Fc**, **Me₂-Fc**, **Me₈-Fc** and **Me₁₀-Fc** in acetonitrile ($c = 1 \cdot 10^{-3}$ M).

On the basis of the electro-optical properties determined for cyanoacrylates and metallocenes, the thermodynamics of the photoinduced electron transfer processes between them to generate the corresponding $CA^{\bullet-}$ and ferrocinium ions (ΔG_{PET}) was evaluated using Rehm-Weller equation.⁹ In all the cases considered, negative ΔG_{PET} values were estimated in acetonitrile solution ($\Delta G_{PET} < -0.3$ eV, Table S2-S3), which were about 0.1, 0.3 and 0.4 eV larger for **Me₂-Fc**, **Me₈-Fc** and **Me₁₀-Fc** with respect to **Fc**. Although slightly less negative figures are expected in the absence of solvent when metallocenes are dissolved in less polar neat cyanoacrylates, our results corroborate the feasibility of light-promoted charge transfer between monomers and photoinitiators, especially for electron-rich ferrocenes. However, it must be noted that the occurrence of PET does not warrant by itself efficient photopolymerization; it is also required that nucleophilic addition of the $CA^{\bullet-}$ species generated on nearby monomers takes place before charge recombination occurs to recover the initial cyanoacrylate and ferrocene compounds.

Cyanoacrylate polymerization with ferrocene-based photoinitiators. As mentioned above, a wide range of cyanoacrylate monomers were explored to evaluate the scope of the ferrocene-based, PET-driven photopolymerization process investigated in this work. Aiming to develop light-curing methodologies that could be used in real applications, we tested the commercial monomer samples as received and no prior purification step was undertaken to remove the radical scavengers (*e.g.* butylated hydroxytoluene) and acids (*e.g.* sulfur dioxide) that are required in CA formulations to prevent premature radical and anionic polymerization, respectively. Although we estimated the amount of acid stabilizers for each monomer by viscosity

acid value determination measurements (t_{AVD} , Table S1),³⁰ it must be noted that the results obtained were biased by the differential reactivity of these compounds. Actually, this explains why the largest t_{AVD} values were found for low-reactivity cyanoacrylates **HCA** and **OCA**.

To assess the efficacy of cyanoacrylate photopolymerization with ferrocene derivatives, calorimetric measurements were performed to enable simple, fast and repetitive *in situ* analysis for multiple monomer-photoinitiator combinations.²⁸ In these experiments very small volumes (100 μ L) of rather diluted metallocene solutions in liquid cyanoacrylate (typically, $0.5 \cdot 10^{-3}$ M) were irradiated with blue light ($\lambda_{exc} = 420$ nm), and the changes in temperature arising from exothermic CA polymerization were monitored. The time at which each sample reached half of the overall thermal increase associated with polymer curing (t_{photo}) was then taken to quantify photopolymerization efficiency, which gives comparable results to other analysis methods (e.g. viscosity or IR measurements (Figure S4)).²⁸

Figures 2 and S5 show the photopolymerization exotherms measured for different CA-metallocene pairs, whereas the corresponding t_{photo} values determined are given in Table 2. When using ferrocene as a photoinitiator, no polymerization was observed for any of the monomers tested even after prolonged irradiation with blue light (30 min), in agreement with previous works that had only reported UV-induced curing of **ECA-Fc** mixtures.^{16,17} However, after a 5-fold increase in **Fc** concentration ($2.5 \cdot 10^{-3}$ M), slow photopolymerization could be achieved for highly reactive **ECA**, thus suggesting the viability of metallocene-based CA curing with visible light. This was further proven when employing methylated ferrocene derivatives with lower oxidation potentials. On one hand, polymerization of not only **ECA** but also **BCA** could be accomplished under continuous blue light illumination with $0.5 \cdot 10^{-3}$ M **Me₂-Fc**, though at rather long time scales (~ 11 -30 min). More interestingly, the use of electron-rich ferrocene

derivatives **Me₈-Fc** and, especially, **Me₁₀-Fc** led to fast CA curing at $c = 0.5 \cdot 10^{-3}$ M and $\lambda_{exc} = 420$ nm even for low-reactivity monomers **HCA** and **OCA**. Actually, solid, tack-free polymeric materials were obtained with these photoinitiators after 2-3 min of blue light illumination in all the cases (Figure 2), which showed no presence of residual, unreacted monomer signals when analyzed by ¹H NMR (Figure S6). By contrast, no polymerization was observed under the same conditions in the dark (or in the absence of the metallocene). In fact, to thermally polymerize small volumes (~ 1 mL) of the cyanoacrylates under study inside non-treated glass vials, they had to be exposed to ambient conditions for several hours (**ECA**) or days (**BCA**, **HCA** and **OCA**), while their mixtures with **Me₈-Fc** and **Me₁₀-Fc** were stable for times that varied from 6 hours (**Me₁₀-Fc** in **ECA**) to 5 days (**Me₈-Fc** in **OCA**) when stored in closed, opaque polypropylene bottles. Therefore, our results demonstrate the capacity of polymethylferrocenes to trigger the photopolymerization of technologically-relevant cyanoacrylates at very mild conditions (i.e. low concentrations, visible light irradiation and fast curing times), thus paving the way to their application for the development of light-curable CA formulations.

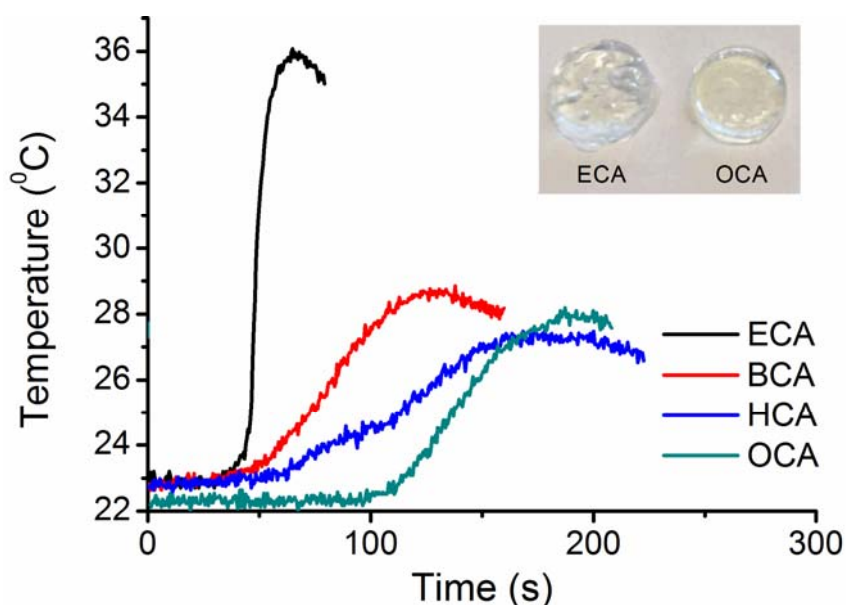


Figure 2. Photopolymerization exotherms of cyanoacrylate monomers containing $0.5 \cdot 10^{-3}$ M **Me₁₀-Fc** ($\lambda_{\text{exc}} = 420$ nm, power = 46 mW cm⁻²). The inset shows photographs of the polymers obtained for **ECA** and **OCA**.

Table 2. Photopolymerization times (t_{photo}) for different monomer-photoinitiator pairs^{a,b,c}

Monomer	Fc	Me ₂ -Fc	Me ₈ -Fc	Me ₁₀ -Fc
ECA	n.o. (719 ± 8 s ^d)	791 ± 5 s	59 ± 1 s	50 ± 3 s
BCA	n.o.	1760 ± 13 s	93 ± 3 s	85 ± 2 s
HCA	n.o.	n.o.	153 ± 6 s	118 ± 3 s
OCA	n.o.	n.o.	164 ± 5 s	140 ± 5 s

n.o. = not observed after 30 min irradiation. ^a Determined as the time at which half of the overall thermal increase is reached for the exotherms registered for each sample while being subjected to continuous irradiation ($\lambda_{\text{exc}} = 420$ nm, power = 46 mW cm⁻²); average of 3 independent measurements. ^b $C_{\text{photoinitiator}} = 0.5 \cdot 10^{-3}$ M. ^c In the absence of irradiation, polymerization of the light-reactive monomer-photoinitiator mixtures was not observed for at least 3 hours. ^d $C_{\text{photoinitiator}} = 2.5 \cdot 10^{-3}$ M.

To evaluate the influence of ferrocene-based photopolymerization on the properties of the cyanoacrylate materials generated, we determined their molecular weight distribution by gel permeation chromatography. In particular, we focused on the case of **Me₁₀-Fc**, with which all the monomers tested could be light-cured, and treated the polymers obtained with acid prior to GPC analysis to prevent depolymerization processes that could affect the molecular weight distributions measured.³² As shown in Table 3 and Figure S7, similar results were found for light- and thermally-cured cyanoacrylates, both in terms of number average molecular weights (M_n) and polydispersities (\mathcal{D}). Actually, for the more relevant monomers **BCA**, **HCA** and **OCA**,

photopolymerization afforded materials with slightly higher M_n and, even better, much lower \mathcal{D} values, an indicator of polymer quality that typically requires faster initiation than propagation processes during polymerization.³⁵ In addition, this demonstrates that no detrimental effects in polymer chain length arise from the much faster polymerization times achieved upon irradiation of the organometallic photoinitiators. Consequently, the excellent adhesive properties of cyanoacrylates must be preserved when applying this photopolymerization technology.

Table 3. Number average molecular weight (M_n , g mol⁻¹) and dispersity (\mathcal{D}) of CA polymers^a

Monomer	Me ₁₀ -Fc photoinitiation	Thermal ^b
ECA	4.00·10 ⁴ (1.97)	5.79·10 ⁴ (2.00)
BCA	5.82·10 ⁵ (1.50)	3.40·10 ⁵ (2.21)
HCA	1.00·10 ⁶ (1.15)	3.08·10 ⁵ (2.63)
OCA	9.67·10 ⁵ (1.15)	3.15·10 ⁵ (2.46)

^a As determined by GPC for freshly prepared polymers, which were photogenerated as described in Table 2; calibration made by using PMMA standards. \mathcal{D} values shown in parentheses. ^b Glass-initiated thermal polymerization under ambient conditions (24 hours).

To corroborate this conclusion, we carried out adhesion tests on poly(methyl methacrylate) (PMMA) substrates, for which we also selected the most active photoinitiator investigated (**Me₁₀-Fc**). In these experiments we determined the maximum tensile strength (σ_{\max}) needed to detach two strips of PMMA previously glued with **ECA**, **BCA** or **OCA** either thermally or photochemically. As shown in Table 4, photoinduced adhesion efficiently took place after just 2 min irradiation for more reactive monomers **ECA** and **BCA** and, in fact, σ_{\max} values measured in this case corresponded to substrate failure instead of adhesive debonding. By contrast, only partial

thermal curing was observed after 30 min with **ECA**, whereas no gluing occurred for **BCA**. Effective thermal adhesion required a much longer period for these two monomers (24 h), only after which mechanical substrate failure was registered in our measurements. As for less-reactive **OCA**, thermal gluing was not achieved even after 24 hours, while photopolymerization with **Me₁₀-Fc** afforded a good adhesion strength after only 2 minutes of blue light illumination, thus again demonstrating the superior curing performance of irradiated CA-metallocene mixtures.

Table 4. Mechanical performance of thermally- and photochemically-cured CA adhesives.

Adhesive	σ_{\max} at 30 min (MPa)^a	σ_{\max} at 24 h (MPa)^a
ECA	1.42 ± 0.48	5.54 ± 0.51 ^c
ECA+Me₁₀-Fc^b	9.38 ± 0.43 ^c	8.29 ± 0.82 ^c
BCA	n. d. ^d	5.02 ± 1.18 ^c
BCA+Me₁₀-Fc^b	5.66 ± 0.39 ^c	5.61 ± 0.60 ^c
OCA	n. d. ^d	n. d. ^d
OCA+Me₁₀-Fc^b	3.33 ± 0.17	2.84 ± 0.28

^a Maximum tensile strength registered 30 min and 24 h after gluing two PMMA plates; average of three replicates. ^b $c_{\text{Me}_{10}\text{-Fc}} = 0.5 \cdot 10^{-3}$ M; irradiation conditions: 420 nm, 46 mW cm⁻², 2 min. ^c σ_{\max} corresponding to substrate failure instead of detachment. ^d not determined because the mix was not cured.

Mechanism of cyanoacrylate polymerization with ferrocene-based photoinitiators. Previous works on the light-induced curing of **ECA** using **Fc** attributed this process to the formation of UV-absorbing charge-transfer (CT) complexes between these two species, the irradiation of which resulted in electron transfer, **CA^{•-}** generation and posterior anionic polymerization.^{16,17} To unravel whether this mechanism also operates when using polymethylferrocenes as photoinitiators, herein we investigated two main aspects: (a) the formation of CT complexes by

interaction between cyanoacrylates and electron-rich ferrocene derivatives; (b) the capacity of $\text{CA}^{\bullet-}$ radical anions to initiate cyanoacrylate anionic polymerization, which had only been proposed theoretically.¹⁸ These studies were mainly conducted on **ECA-Me₁₀-Fc** mixtures, the most reactive monomer-photoinitiator pair identified in this work.

As discussed above, photoinduced electron transfer between **ECA** and **Me₁₀-Fc** (as well as for the rest of CA monomers and metallocenes tested) must be thermodynamically allowed under blue light irradiation based on the electro-optical properties of these compounds. This implies that, after photoexcitation of **Me₁₀-Fc**, an electron can be transferred from its excited state towards **ECA** molecules provided that they lie in the close vicinity, a very plausible hypothesis for metallocene solutions in neat cyanoacrylate. Alternatively, if nearby **ECA** and **Me₁₀-Fc** molecules are strongly electronically coupled, CT complexes can also be formed, the excitation of which directly leads to electron transfer and formation of $\text{ECA}^{\bullet-}$ and $\text{Me}_{10}\text{-Fc}^+$ ions. Because these complexes present characteristic absorption bands that differ from those of their separate constituting units,³⁴ we investigated the spectral changes occurring when dissolving **Me₁₀-Fc** in **ECA** (Figure 3). Two main differences were observed with respect to metallocene solutions in standard organic solvents, which can be ascribed to the formation of CT complexes between ferrocenes and electron acceptors³⁴ (e.g. 1,4-quinone derivatives³⁶ or tetracyanoethylene³⁷): (a) broadening and increase in the intensity of the absorption band at $\lambda_{\text{abs,max}} \sim 420$ nm arising from **Me₁₀-Fc**, and (b) appearance of a new absorption peak at $\lambda_{\text{abs,max}} \sim 790$ nm. Interestingly, the latter resembles the absorption of $\text{Me}_{10}\text{-Fc}^+$ in the near-infrared region of the spectrum (Figure S8), a behavior that is typically attributed to ferrocene-electron acceptor complexes where radical-ion pair formation is favored after electron transfer.³⁷

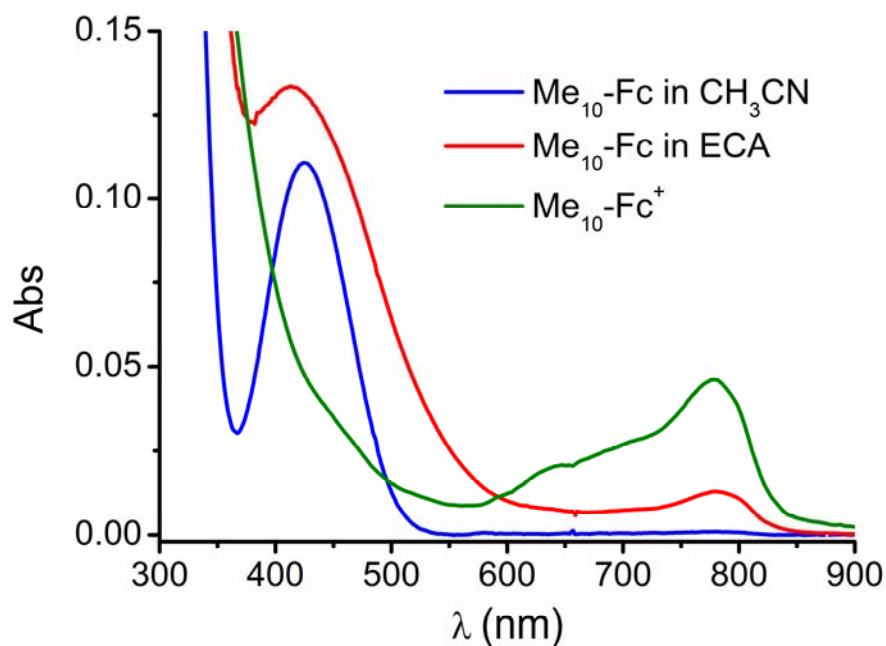


Figure 3. Absorption spectra of **Me₁₀-Fc** in neat acetonitrile ($c = 1 \cdot 10^{-3}$ M) and after adding an excess of **ECA** ($c = 0.6$ M).

Similar spectral features were registered for most of the polymethylferrocene-cyanoacrylate pairs that underwent photopolymerization in this work (Figure S9). Based on this absorption data and assuming a 1:1 stoichiometry, the formation constants (K_a) for the complexes formed between these electron-donating and electron-accepting species were determined by means of the Benesi-Hildebrand method (Table S4).³⁷ As previously reported for other ferrocene-electron acceptor mixtures,³⁷ rather small values were found in all the cases ($K_a < 0.5 \text{ M}^{-1}$), which however fairly correlated with the photopolymerization results: the larger K_a , the shorter t_{photo} . Actually, it must be noted that, at the high concentrations employed in the photopolymerization experiments (i.e. neat cyanoacrylate), a significant fraction of the photoinitiating ferrocene molecules are expected to be involved in the formation of charge-transfer complexes with cyanoacrylate monomers despite the low K_a values estimated (up to 57% for **ECA-Me₁₀-Fc**,

Table S4). As such, they should play a crucial role in the light-induced polymerization processes observed.

To further confirm this conclusion, photopolymerization of **ECA-Me₁₀-Fc** mixtures was attempted at $\lambda_{\text{exc}} = 780$ nm, a near-infrared wavelength that is not absorbed by the metallocene but only by the species derived from CT complex formation. Remarkably, light-induced cyanoacrylate curing also took place under these illumination conditions, although with a longer time with respect to blue light irradiation that we mainly ascribed to the lower absorption at 780 nm ($t_{\text{photo}} = 281$ s, Figure S10). This result does not only support the assignment of ferrocene-induced photopolymerization of cyanoacrylates to photoinduced electron transfer, but also opens new avenues to the application of this technology, since excitation with IR light is highly preferred for many uses due to its larger penetration depth into materials with lower photodamage.³⁸ Actually, to our knowledge, this work constitutes the first report of CA light-curing accomplished with near-infrared radiation.

Once proven the occurrence of PET between **ECA** and **Me₁₀-Fc**, we also investigated whether the **CA^{•-}** radical anions generated through this process could trigger cyanoacrylate anionic polymerization, as suggested by theoretical calculations.¹⁸ In a first step, we conducted electrolytic experiments to demonstrate the capacity to induce **ECA** curing under reductive conditions (i.e. upon electrochemical generation of **ECA^{•-}**). Interestingly, when a controlled potential electrolysis at -2.1 V (vs SCE) was performed, the formation of a thin layer of an off-white material onto the working electrode was observed after the passage of 1 *F*, which we found to consist of a mixture of low-molecular weight **ECA** polymers and the supporting electrolyte used (Figure S11). Therefore, this uncovered the feasibility of initiating cyanoacrylate polymerization by means of **ECA^{•-}** ions.

Next, we focused on the analysis of the polymerization mechanism for this process. For this, we carried out new light-induced curing experiments with increasing amounts of a strong acid (methanesulfonic acid, MSA), which can inhibit both the anionic initiating species and the reactive anionic sites on polymers by protonation. As shown in Figure 4, very small additions of MSA (~ few ppm) drastically slowed down the photopolymerization reaction, thus demonstrating that it proceeded through an anionic mechanism (Scheme S1). Actually, when analogous measurements were performed using a radical scavenger (butylated hydroxyanisole, BHA), much larger quantities were required to observe a detrimental effect on light-curing efficiency (~ thousands of ppm, Figure S12), which allowed us corroborating: (a) the very minor contribution of the radical mechanism to the polymerization process, as expected from the experiments performed with MSA; (b) the radical nature of the actual initiating species of cyanoacrylate curing (i.e. ECA^\bullet), which may be eventually quenched by addition of high concentrations of radical stabilizers. It must be noted that, however, such species cannot prevent propagation reactions on the anionic sites of polymer chains, since they become increasingly separated from the radical sites as the system grows (Scheme S1). Therefore, interaction between the radical sites in growing polymers and radical scavengers should not inhibit polymerization by anion addition on new monomers.

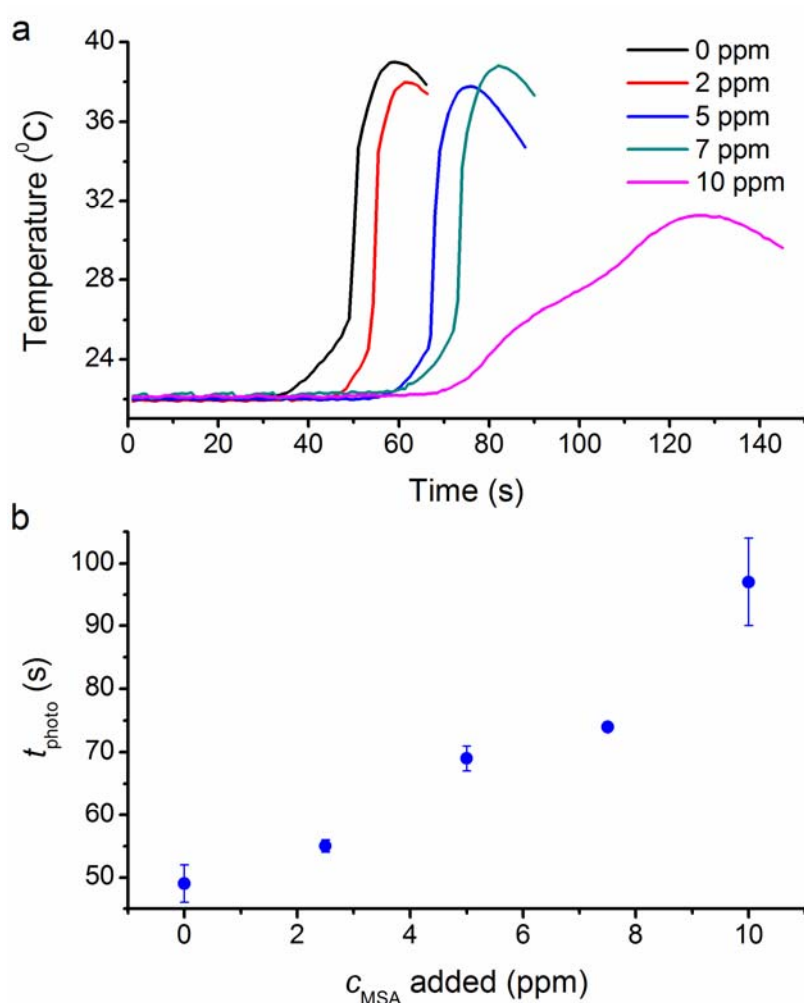
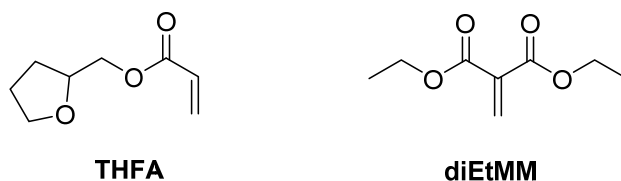


Figure 4. (a) Photopolymerization exotherms of **ECA** containing $0.5 \cdot 10^{-3}$ M **Me₁₀-Fc** ($\lambda_{\text{exc}} = 420$ nm, power = 46 mW cm^{-2}) and increasing amounts of an acid stabilizer (methanesulfonic acid, added from a 50 ppm stock solution in neat **ECA**). (b) Variation of t_{photo} in these experiments with the concentration of MSA added.

Generalization of ferrocene-based photoinitiation to other monomers. In view of the capacity of polymethylferrocenes to provide fast photoinduced curing of cyanoacrylates with visible (and even infrared) light, we explored the use of this technology to other monomers. Because of the double radical and anionic nature of the initiating species produced in this case (e.g. **ECA^{••}**),

both radical and anionic polymerizations could in principle be realized. However, an important requirement must be met by the reactive monomers: they should present electron-deficient olefins capable to undergo photoinduced electron transfer with electron-rich ferrocenes. For this reason we focus our attention on acrylate monomers, where the presence of one (or more) electron-withdrawing ester groups may decrease their reduction potential enough as to favor PET with the best of the photoinitiators established in this work (**Me₁₀-Fc**). In particular, we tested two different monomers: (a) tetrahydrofurfuryl acrylate (**THFA**), a regular acrylate monomer that is known to polymerize via a radical mechanism;³⁹ (b) diethyl methylenemalonate (**diEtMM**) bearing two ester groups connected to its carbon-carbon double bond, which favors nucleophilic conjugated addition and, as such, anionic polymerization⁴⁰ (Scheme 2). In addition, the bisoxycarbonyl substitution pattern of **diEtMM** significantly reduces its reduction potential with respect to **THFA** ($E_{\text{red}} = -1.74$ and -2.19 V vs SCE in acetonitrile, respectively; Figure S13), thus making its electrochemical behavior more similar to that of CA monomers ($E_{\text{red}} \sim -1.6$ vs SCE). Nonetheless, photoinduced electron transfer from **Me₁₀-Fc** to **diEtMM** and **THFA** is expected to be thermodynamically favored in both cases ($\Delta G_{\text{PET}} = -0.74$ and -0.29 eV in acetonitrile, respectively).



Scheme 2 Acrylate monomers tested to accomplish PET-induced polymerization using polymethylferrocenes.

Calorimetric studies were conducted to test the photopolymerization of **THFA** and **diEtMM** using **Me₁₀-Fc** under blue light irradiation ($\lambda_{\text{exc}} = 420$ nm). In the case of **THFA** no light-induced curing was observed, not even under very long irradiation times (up to 3000 s), large photoinitiator concentrations (up to $30 \cdot 10^{-3}$ M) or after purifying the commercially received monomer to minimize the amount of radical stabilizers in the reaction mixture. Two main factors could account for this result: (a) the less favorable reduction potential of **THFA**, which must reduce its capacity to undergo electron transfer with **Me₁₀-Fc** under irradiation and favor the reverse charge recombination process, thus decreasing the concentration and lifetime of **THFA**^{•-} ions; (b) the poor (or no) reactivity of these ions with **THFA** monomers via a radical addition mechanism, which should initiate the polymerization process.

By contrast, ferrocene-induced photopolymerization was achieved for **diEtMM**, which resulted in tack-free polymer materials with similar molecular weight distributions to those obtained thermally (Figures 5 and S14-15). In this case, however, larger photoinitiator concentrations ($c_{\text{Me}_{10}\text{-Fc}} = 30 \cdot 10^{-3}$ M) and illumination times ($t_{\text{photo}} = 431 \pm 29$ s) were required with respect to cyanoacrylates. We mainly attributed this behavior to: (a) the lower reactivity of **diEtMM** in nucleophilic conjugated addition processes, as already reported⁴⁰ and illustrated by the very high t_{AVD} value determined for the particular monomer sample used in our work ($t_{\text{AVD}} > 3600$ h, Table S1); (b) the lower electronic interaction with ferrocene molecules, as revealed by the absence of spectral features in the absorption spectrum of **diEtMM-Me₁₀-Fc** mixtures that were indicative of charge-transfer complex formation. In addition, because of the slightly larger reduction potential of **diEtMM** with respect to cyanoacrylates, charge recombination to recover the initial **diEtMM** and **Me₁₀-Fc** species after PET must be more favored in this case, thus strongly competing with the slow addition of **diEtMM**^{•-} to monomers to start the polymerization

reaction. In spite of this, our results demonstrate that electron-rich polymethylferrocenes can be applied to light-cure electron-deficient olefins other than cyanoacrylates with visible radiation, thus broadening the scope of the photopolymerization technology introduced in this work.

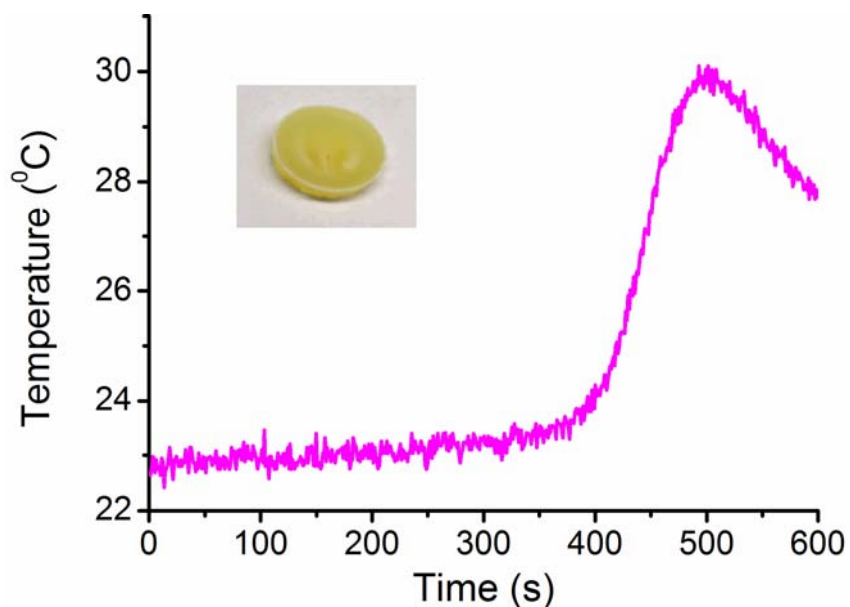


Figure 5. Photopolymerization exotherm of **diEtMM** containing 30 mM **Me₁₀-Fc** ($\lambda_{\text{exc}} = 420$ nm, power = 46 mW cm⁻²). The inset shows a photograph of the polymer material obtained.

CONCLUSIONS

In this work we described a new strategy to accomplish cyanoacrylate photopolymerization based on the use of electron-rich polymethylferrocenes. Upon irradiation of these compounds, radical anions of the cyanoacrylate monomers are formed by electron transfer that are capable to initiate the polymerization reaction. In this way, very fast, on demand polymer curing was achieved even for poorly reactive, but biologically-relevant long alkyl chain cyanoacrylates using low intensity visible light and photoinitiator loadings ($< 1 \cdot 10^{-3}$ M). This is in contrast to the

photoinitiator behavior so far reported for other metallocenes, which only allowed polymerization of highly reactive cyanoacrylates by means of UV radiation and rather long illumination times. Actually, for the most active photoinitiator identified herein, cyanoacrylate photopolymerization could be accomplished for the first time with near-infrared light, while it could also be successfully applied to photocure other electron-deficient, non-cyanoacrylate monomers. No detrimental effects on the molecular weight of the resulting polymer materials obtained were observed, which preserved their superior adhesive properties. These excellent features, in combination with the low cost or ease of preparation of the initiators, make the photopolymerization strategy developed in this work very promising for the development of high-performance, light-curable formulations of cyanoacrylate (and other) adhesives for practical applications (e.g. in the biomedical field).

ASSOCIATED CONTENT

Supporting Information. Additional data on the synthesis of the photoinitiator **Me₈-Fc**, the electro-optical characterization of monomers and photoinitiators, and the polymerization and characterization of polymers. This material is available free of charge via the Internet at <http://pubs.acs.org>.

AUTHOR INFORMATION

Corresponding Author

* (J.H.) E-mail: jordi.hernando@uab.cat

* (R.M.S.) E-mail: rosamaria.sebastian@uab.cat

Author Contributions

The manuscript was written through contributions of all authors. All authors have given approval to the final version of the manuscript.

ACKNOWLEDGEMENTS

Financial support by MINECO/FEDER (RTC-2016-5683-1 project within "Retos Colaboración" program and CTQ2015-65439-R project) and by Generalitat de Catalunya (2017 SGR00465 project) is gratefully acknowledged. C. G. thanks MINECO for her FPI doctoral fellowship (BES-2016-078179).

ABBREVIATIONS

PET, photoinduced electron transfer; CA, cyanoacrylate; Fc, ferrocene; Me₂-Fc, 1,1'-dimethylferrocene; Me₈-Fc, octamethylferrocene; Me₁₀-Fc, decamethylferrocene; ECA, ethyl 2-cyanoacrylate; BCA, butyl 2-cyanoacrylate; HCA, hexyl 2-cyanoacrylate; OCA, 2-octyl 2-cyanoacrylate; WE, working electrode; CE, auxiliary electrode; SCE, saturated calomel reference electrode; AVD, acid value determination; t_{photo} , photopolymerization time; GPC, gel permeation chromatography; Mn, number average molecular weight; MSA, methanesulfonic acid; PMMA, poly(methyl methacrylate); BHA, butylated hydroxyanisole; THFA, tetrahydrofurfuryl acrylate; diEtMM, diethyl methylenemalonate.

REFERENCES

- (1) Photopolymerization: Fundamentals and Applications. Scranton, A. B., Bowman, C. N., Peiffer, R. W., Eds.; ACS Symposium Series No. 673; American Chemical Society: Washington, 1997.
- (2) Yagci, Y.; Jockush, S.; Turro, N. J. Photoinitiated Polymerization: Advances, Challenges, and Opportunities. *Macromolecules* **2010**, *43*, 6245-6260.
- (3) Chatani, S.; Kloxin, C. J.; Bowman, C. N. The Power of Light in Polymer Science: Photochemical processes to Manipulate Polymer Formation, Structure, and Properties. *Polym. Chem.* **2014**, *5*, 2187–2201.
- (4) Michaudel, Q.; Kottisch, V.; Fors, B. P. Cationic Polymerization: From Photoinitiation to Photocontrol. *Angew. Chem. Int. Ed.* **2017**, *56*, 9670-9679.
- (5) Ikemura, K.; Endo, T. A Review of the Development of Radical Photopolymerization Initiators Used for Designing Light-Curing Dental Adhesives and Resin Composites. *Dent. Mater. J.* **2010**, *29*, 481-501.
- (6) Ligon, S. C.; Liska, R.; Stampfl, J.; Gurr, M.; Mühlaupt, R. Polymers for 3D Printing and Customized Additive Manufacturing. *Chem. Rev.* **2017**, *117*, 10212-10290.
- (7) Zhang, J.; Xiao, P. 3D Printing of Photopolymers. *Polym. Chem.* **2018**, *9*, 1530-1540.
- (8) Vitale, A.; Trusiano, G.; Bongiovanni, R. In *Progress in Adhesion and Adhesives*. Mittal K. L., Ed.; Scrivener Publishing LLC: Beverly, 2015, pp. 56-96.
- (9) Dadashi-Silab, S.; Doran, S.; Yagci, Y. Photoinduced Electron Transfer Reactions for Macromolecular Syntheses. *Chem. Rev.* **2016**, *116*, 10212-10275.
- (10) Fink, J. K. In *Reactive Polymers Fundamentals and Applications*, 2nd ed.; William Andrew Publishing: Norwich, 2013; pp. 317-330.
- (11) Burns, B. Polycyanoacrylates. In *Encyclopedia of Polymer Science and Technology*, 4th ed.; John Wiley & Sons: Hoboken, 2016; Volume 4, pp. 1–27.
- (12) Shantha, K. L.; Thennarasu, S.; Krishnamurti, N. Developments and applications of cyanoacrylate adhesives. *J. Adh. Sci. Tech.* **1989**, *3*, 237-260.

- (13) Petrie, E. M. Cyanoacrylate Adhesives in Surgical Applications. In *Progress in Adhesion and Adhesives*, 1st ed.; Mittal, K. L., Ed.; Scrivener Publishing LLC: Beverly, 2015; pp. 245-298.
- (14) Herod, E. Cyanoacrylates in Dentistry: a Review of the Literature. *J. Can. Dental Assoc.* **1990**, *56*, 331-334.
- (15) Papay, K. L. Vitamin/Mineral-Enriched Cyanoacrylate Cosmetic, U.S. Patent 5,866,106A, February 2, 1999.
- (16) Sanderson, C. T.; Palmer, B. J.; Morgan, A.; Murphy, M.; Dluhy, R. A.; Mize, T.; Amster, J.; Kutal, C. Classical Metallocenes as Photoinitiators for the Anionic Polymerization of an Alkyl 2-Cyanoacrylate. *Macromolecules* **2002**, *35*, 9648-9652.
- (17) Yamaguchi, Y.; Ding, W.; Sanderson, C. T.; Borden, M. L.; Morgan, M. J.; Kutal, C. Electronic Structure, Spectroscopy, and Photochemistry of Group 8 Metallocenes. *Coord. Chem. Rev.* **2007**, *251*, 515-524.
- (18) Brinkmann, N. R.; Schaefer III, H. F.; Sanderson, C. T.; Kutal, C. Can the Radical Anion of Alkyl-2-cyanoacrylates Initiate Anionic Polymerization of These Instant Adhesive Monomers? *J. Phys. Chem. A* **2002**, *106*, 847-853.
- (19) Patra, M.; Gasser, G. The Medicinal Chemistry of Ferrocene and its Derivatives. *Nat. Rev. Chem.* **2017**, *1*, 0066.
- (20) Kutal, C.; Grutsch, P. A.; Yang, D. B. A Novel Strategy for Photoinitiated Anionic Polymerization. *Macromolecules* **1991**, *24*, 6872-6873.
- (21) Paul, R. B.; Kelly, J. M.; Pepper, D. C.; Long, C. Photoinduced Anionic Polymerization of Cyanoacrylates using Substituted Pyridine Pentacarbonyl Complexes of Tungsten or Chromium. *Polymer* **1997**, *38*, 2011-2014.
- (22) Palmer, B. J.; Kutal, C.; Billing, R.; Hennig, H. A New Photoinitiator for Anionic Polymerization. *Macromolecules* **1995**, *28*, 1328-1329.
- (23) Yamaguchi, Y.; Palmer, B. J.; Kutal, C.; Wakamatsu, T.; Yang, D. B. Ferrocenes as Anionic Photoinitiators. *Macromolecules* **1998**, *31*, 5155-5157.

- (24) Yamaguchi, Y.; Kutal, C. Benzoyl-Substituted Ferrocenes: An Attractive New Class of Anionic Photoinitiators. *Macromolecules* **2000**, *33*, 1152-1156.
- (25) Arsu, N.; Önen, A.; Yagci, Y. Photoinitiated Zwitterionic Polymerization of Alkyl Cyanoacrylates by Pyridinium Salts. *Macromolecules* **1996**, *29*, 8973-8974.
- (26) Önen, A.; Arsu, N.; Yagci, Y. Photoinitiated Polymerization of Ethyl Cyanoacrylate by Phosphonium Salts. *Angew. Makromol. Chem.* **1999**, *264*, 56-59.
- (27) Jarikov, V. V.; Neckers, D. C. Anionic Photopolymerization of Methyl 2-Cyanoacrylate and Simultaneous Color Formation. *Macromolecules* **2000**, *33*, 7761-7764.
- (28) Faggi, E.; Aguilera, J.; Sáez, R.; Pujol, F.; Marquet, J.; Hernando, J.; Sebastián, R. M. Wavelength-Tunable Light-Induced Polymerization of Cyanoacrylates Using Photogenerated Amines. *Macromolecules* **2019**, *52*, 2329–2339.
- (29) Roemer, M.; Skelton, B. W.; Piggott, M. J.; Koutsantonis, G. A. 1,1'-Diacetyloctamethylferrocene: an overlooked and overdue synthon leading to the facile synthesis of an octamethylferrocenophane. *Dalton Trans.* **2016**, *45*, 18817-18821.
- (30) Cooke, B. D.; Allen, K. W. Cyanoacrylates and their Acid Values, *Int. J. Adhesion Adhesives* **13**, **1993**, 73-76.
- (31) Szanka, I.; Szanka, A.; Kennedy, J. P. Rubbery Wound Closure Adhesives. II. Initiators for and Initiation of 2-Octyl Cyanoacrylate Polymerization. *J. Polym. Sci., Part A: Polym. Chem.* **2015**, *53*, 1652-1659.
- (32) Robello, D. R.; Eldridge, T. D.; Swanson, M. T. Degradation and Stabilization of Polycyanoacrylates, *J. Polym. Sci., Part A: Polym. Chem.* **1999**, *37*, 4570-4581.
- (33) Duffy, C.; Zetterlund, P. B.; Aldabbagh, F. Radical Polymerization of Alkyl 2-Cyanoacrylates. *Molecules* **2018**, *23*, 465.
- (34) Togni, A. In *Ferrocenes*. Togni, A.; Hayashi, T. Eds.; VCH: Weinheim, 1995, pp. 433-466.
- (35) Sáez, R.; McArdle, C.; Salhi, F.; Marquet, J.; Sebastián, R. M. Controlled Living Anionic Polymerization of Cyanoacrylates by Frustrated Lewis Pair Based Initiators. *Chem. Sci.* **2019**, *10*, 3295-3299.

(36) Mochida, T.; Funasako, Y.; Azumi, H. Charge-transfer complexes from decamethylferrocene and 1,4-quinone derivatives: neutral–ionic phase diagrams for metallocene complexes. *Dalton Trans.* **2011**, *40*, 9221-9228.

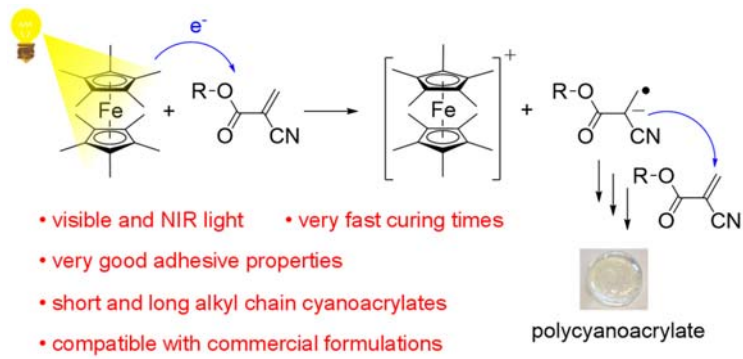
(37) Frey, J. E.; Du Pont, L. E.; Puckett, J. J. Formation Constants of Radical-Ion Pairs and Charge-Transfer Complexes of Tetracyanoethylene with Group 8 Metallocenes. *J. Org. Chem.* **1994**, *59*, 5386-5392.

(38) Bonardi, A. H.; Dumur, F.; Grant, T. M.; Noirbent, G.; Gimes, D.; Lessard, B. H.; Fouassier, J.-P.; Lalevée, J. High Performance Near-Infrared (NIR) Photoinitiating Systems Operating under Low Light Intensity and in the Presence of Oxygen. *Macromolecules* **2018**, *51*, 1314-1324.

(39) Lu, W.; Wang, Y.; Wang, W.; Cheng, S.; Zhu, J.; Xu, Y.; Hong, K.; Kang, N.-G.; Mays, J. All Acrylic-Based Thermoplastic Elastomers with High Upper Service Temperature and Superior Mechanical Properties. *Polym. Chem.* **2017**, *8*, 5741-5748.

(40) Klemarczyk, P. A General Synthesis of 1,1 Disubstituted Electron Deficient Olefins and their Polymer Properties. *Polymer* **1998**, *39*, 173–181.

Table of contents graphic



Supporting Information for:

Polymethylferrocene-induced
photopolymerization of cyanoacrylates using
visible and near-infrared light

Enrico Faggi,^a Carolina Gascó,^a Jordi Aguilera,^b Gonzalo Guirado,^a Sara Ortego,^b Rubén Sáez,^b Ferran Pujol,^b Jordi Marquet,^a Jordi Hernando,^{a,} and Rosa María Sebastián^{a,*}*

^a Departament de Química, Universitat Autònoma de Barcelona, Cerdanyola del Vallès,
Spain

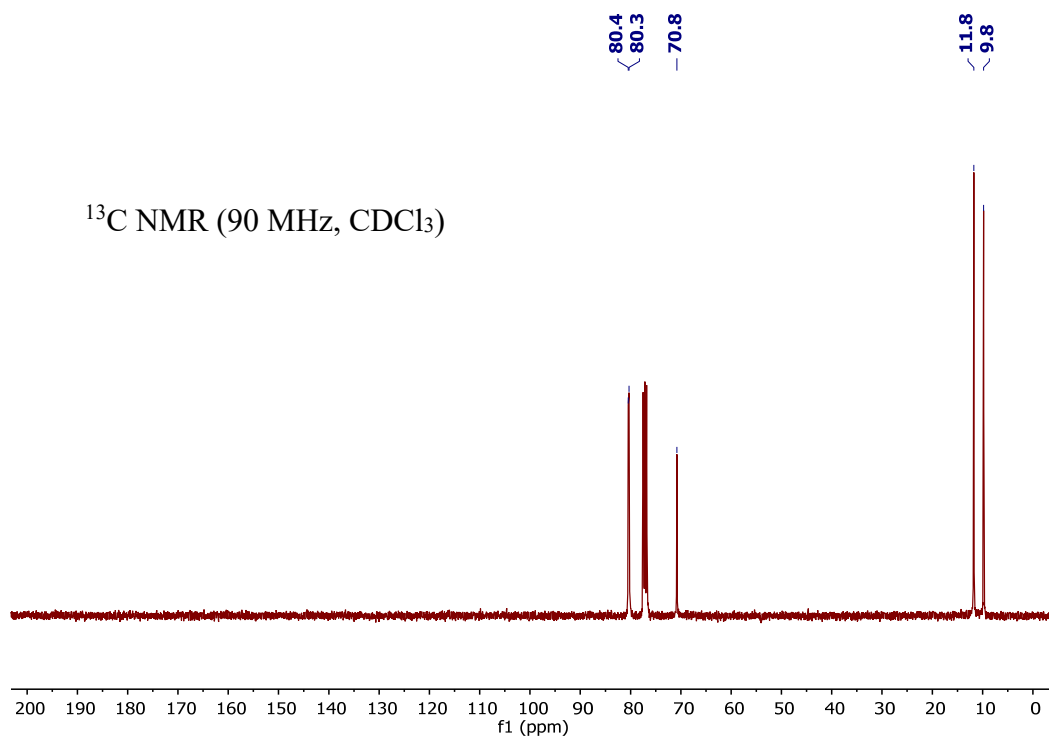
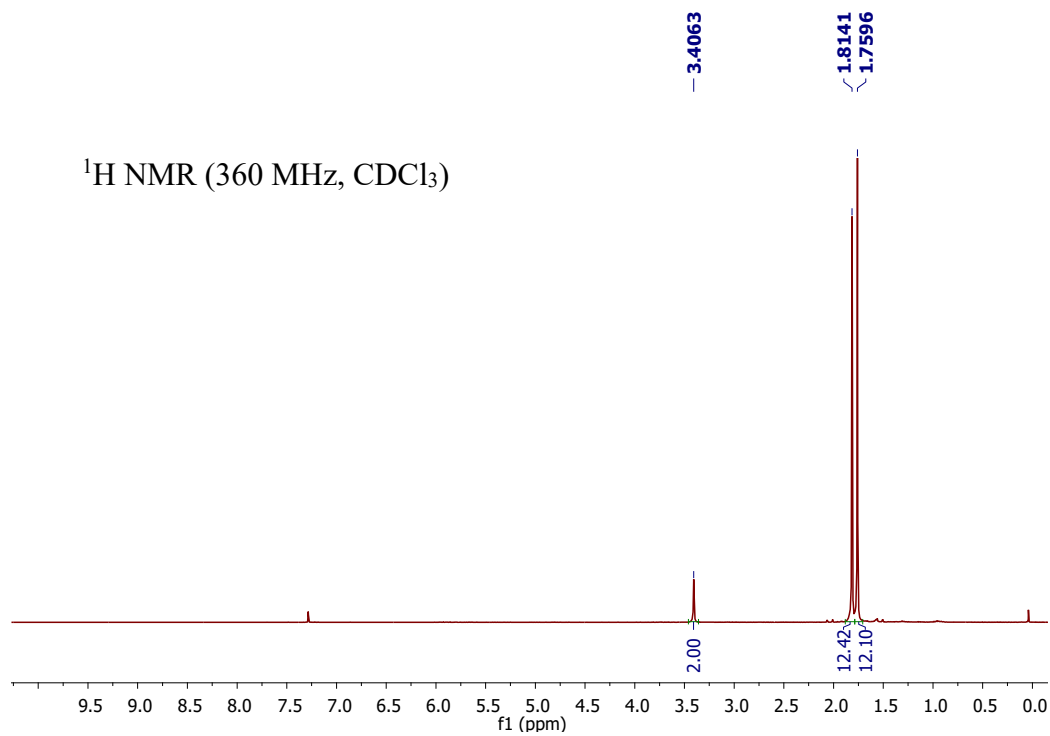
^b CUANTUM Medical Cosmetics S.L., Cerdanyola del Vallès, Spain

TABLE OF CONTENTS:

1. ¹H NMR AND ¹³C NMR SPECTRA OF PHOTOINITIATOR Meg-Fc.....	S3
2. TOTAL ACID DETERMINATION OF CYANOACRYLATE MONOMERS..	S4
3. ELECTRO-OPTICAL PROPERTIES OF CYANOACRYLATES.....	S5
4. OPTICAL PROPERTIES OF PHOTOINITIATORS.....	S6
5. PHOTOINDUCED ELECTRON TRANSFER BETWEEN CYANOACRYLATE MONOMERS AND PHOTOINITIATORS.....	S7
6. PHOTOPOLYMERIZATION OF CYANOACRYLATE MONOMERS.....	S9
7. MECHANISM OF PHOTOPOLYMERIZATION.....	S13
8. PHOTOPOLYMERIZATION OF OTHER MONOMERS.....	S18
9. REFERENCES.....	S20

1. ^1H NMR AND ^{13}C NMR SPECTRA OF PHOTOINITIATOR $\text{Me}_8\text{-Fc}$

^1H NMR and ^{13}C NMR spectra are shown for $\text{Me}_8\text{-Fc}$, which perfectly agree with previously reported data.¹



2. TOTAL ACID DETERMINATION OF CYANOACRYLATE MONOMERS

Table S1. Viscosity acid value determination² of CA monomers

Monomer	t_{AVD} (s)
ECA	88
BCA	130
HCA	670
OCA	505
diEtMM	> 3600

3. ELECTRO-OPTICAL PROPERTIES OF CYANOACRYLATES

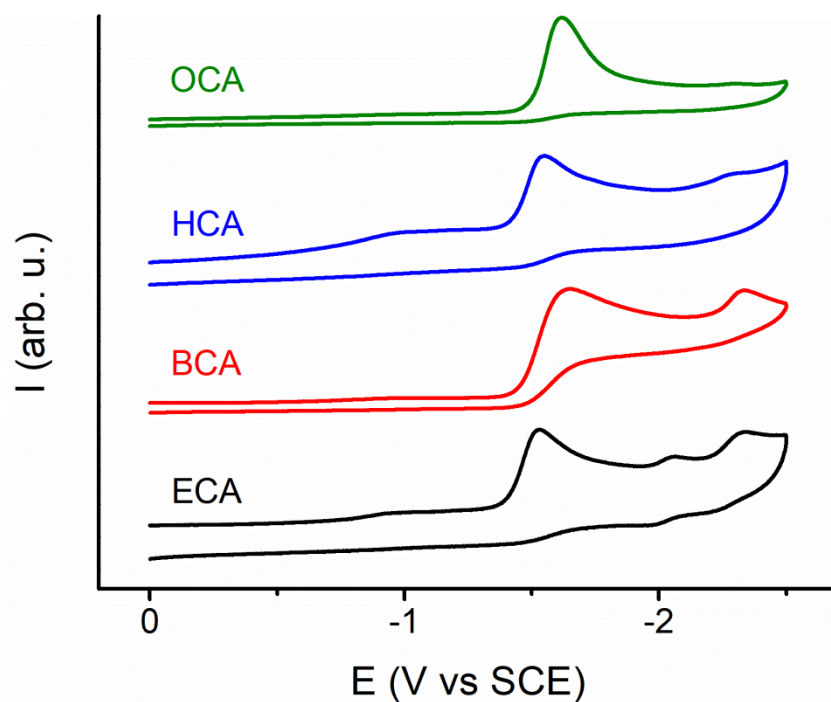


Figure S1. Cyclic voltammograms of **ECA**, **BCA**, **HCA** and **OCA** ($c \sim 6 \cdot 10^{-3}$ M) in acetonitrile (+ 0.1 M *n*-Bu₄NPF₆; scan rate 0.5 V s⁻¹).

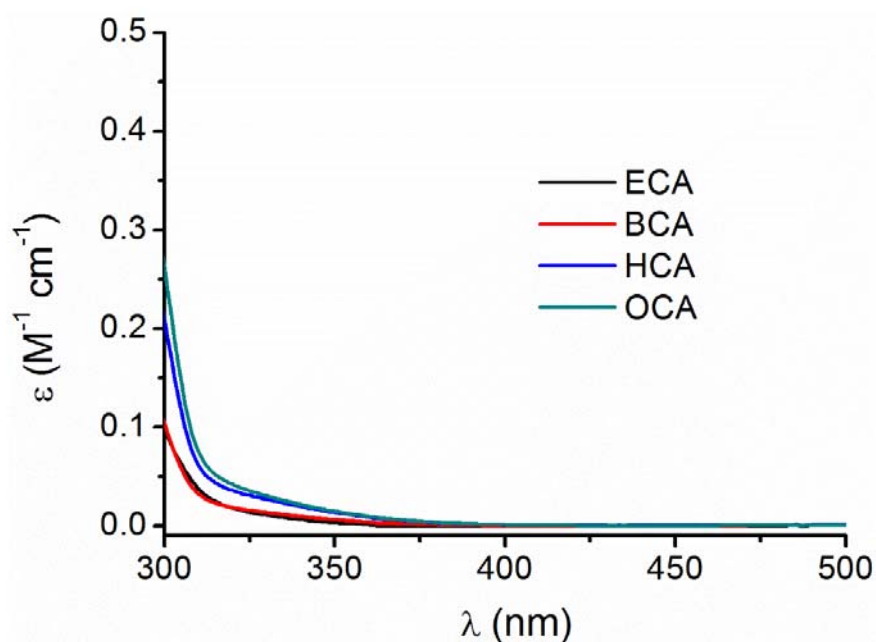


Figure S2. Absorption spectra of neat **ECA**, **BCA**, **HCA** and **OCA**.

4. OPTICAL PROPERTIES OF PHOTOINITIATORS

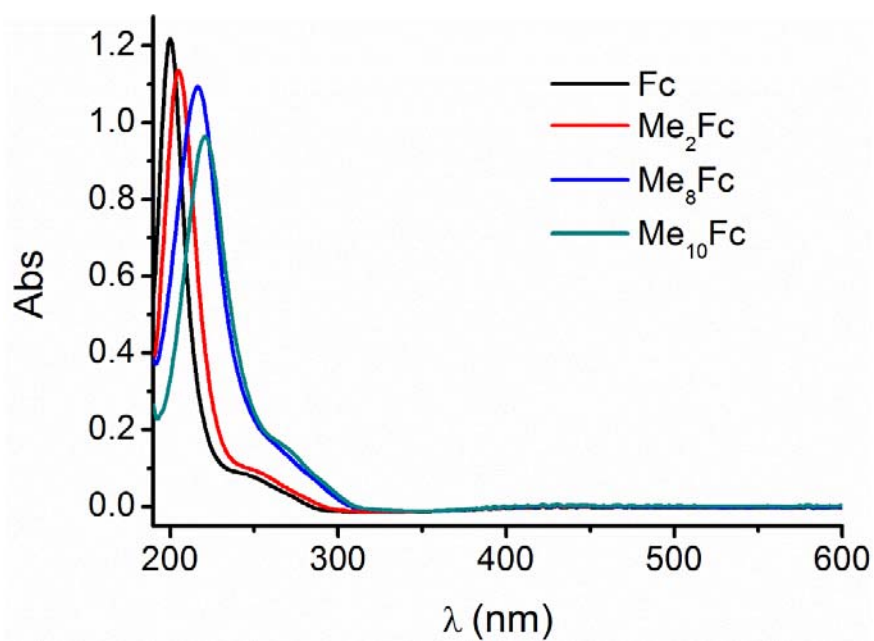


Figure S3. Absorption spectra of **Fc**, **Me₂-Fc**, **Me₈-Fc** and **Me₁₀-Fc** ($c = 4 \cdot 10^{-5}$ M) in acetonitrile.

5. PHOTOINDUCED ELECTRON TRANSFER BETWEEN CYANOACRYLATE MONOMERS AND PHOTOINITIATORS

Table S2. Excitation energies (E_{00}) and excited state oxidation potentials (E^*_{ox}) in acetonitrile of the different ferrocene photoinitiators investigated

	E_{00} (eV) ^a	E^*_{ox} (V vs SCE) ^b
Fc	2.21	-1.71
Me₂-Fc	2.21	-1.97
Me₈-Fc	2.25	-2.31
Me₁₀-Fc	2.25	-2.40

^a Since neither ferrocene nor polymethylferrocenes are fluorescent, E_{00} values were estimated from the low-energy onset of their absorption band in the visible region. ^b Determined as $E_{ox} - E_{00}$.

Table S3. ΔG_{PET} (in eV) in acetonitrile for the different CA monomer-photoinitiator pairs investigated^a

	Fc	Me₂-Fc	Me₈-Fc	Me₁₀-Fc
ECA	-0.37	-0.51	-0.85	-0.94
BCA	-0.26	-0.40	-0.74	-0.83
HCA	-0.36	-0.50	-0.84	-0.93
OCA	-0.29	-0.43	-0.77	-0.86

^a Values determined using equation S1,³ where: $E_{ox}(D)$ is the oxidation potential of the metallocene for the metallocinium/metallocene couple, which we took as the half-wave value experimentally determined in acetonitrile; $E_{red}(A)$ is the reduction potential of the cyanoacrylate monomers, which we took as the cathodic peak potential value experimentally determined in acetonitrile; E_{00} is the excitation energy of the metallocene in acetonitrile (see Table S2); ϵ_s is the relative permittivity of acetonitrile;

R_{cc} is the center-to-center distance between the metallocene and the cyanoacrylate monomer, which we assumed to be 0.5 nm as an approximation.

$$\Delta G_{\text{PET}} = e(E_{\text{ox}}(\text{D}) - E_{\text{red}}(\text{A})) - E_{00} - \frac{e^2}{4\pi\epsilon_0\epsilon_s R_{cc}} \quad (\text{S1})$$

6. PHOTOPOLYMERIZATION OF CYANOACRYLATE MONOMERS

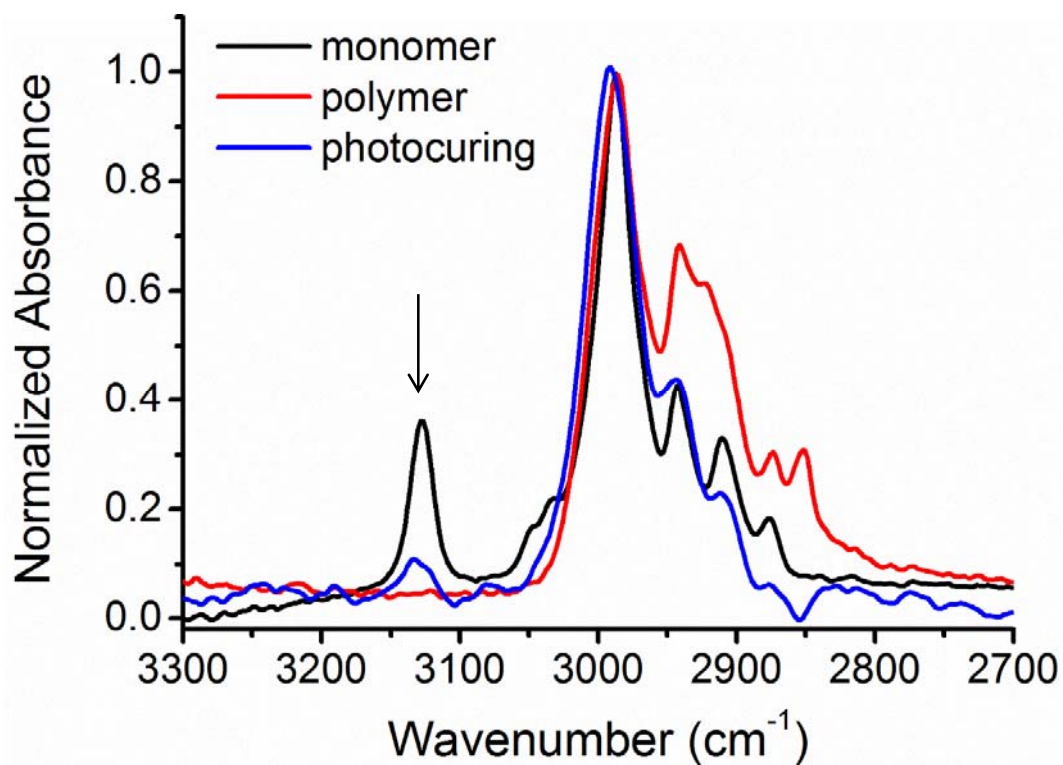


Figure S4. IR spectra of ECA monomer, a fully cured ECA+Me₁₀-Fc mixture and an ECA+Me₁₀-Fc mixture at $t_{\text{photo}} = 50$ s. The arrow shows the peak at 3128 cm⁻¹, which decreases as polymerization takes place. By integrating the area of this peak, we could estimate that about 80% of the initial monomer had polymerized by t_{photo} .

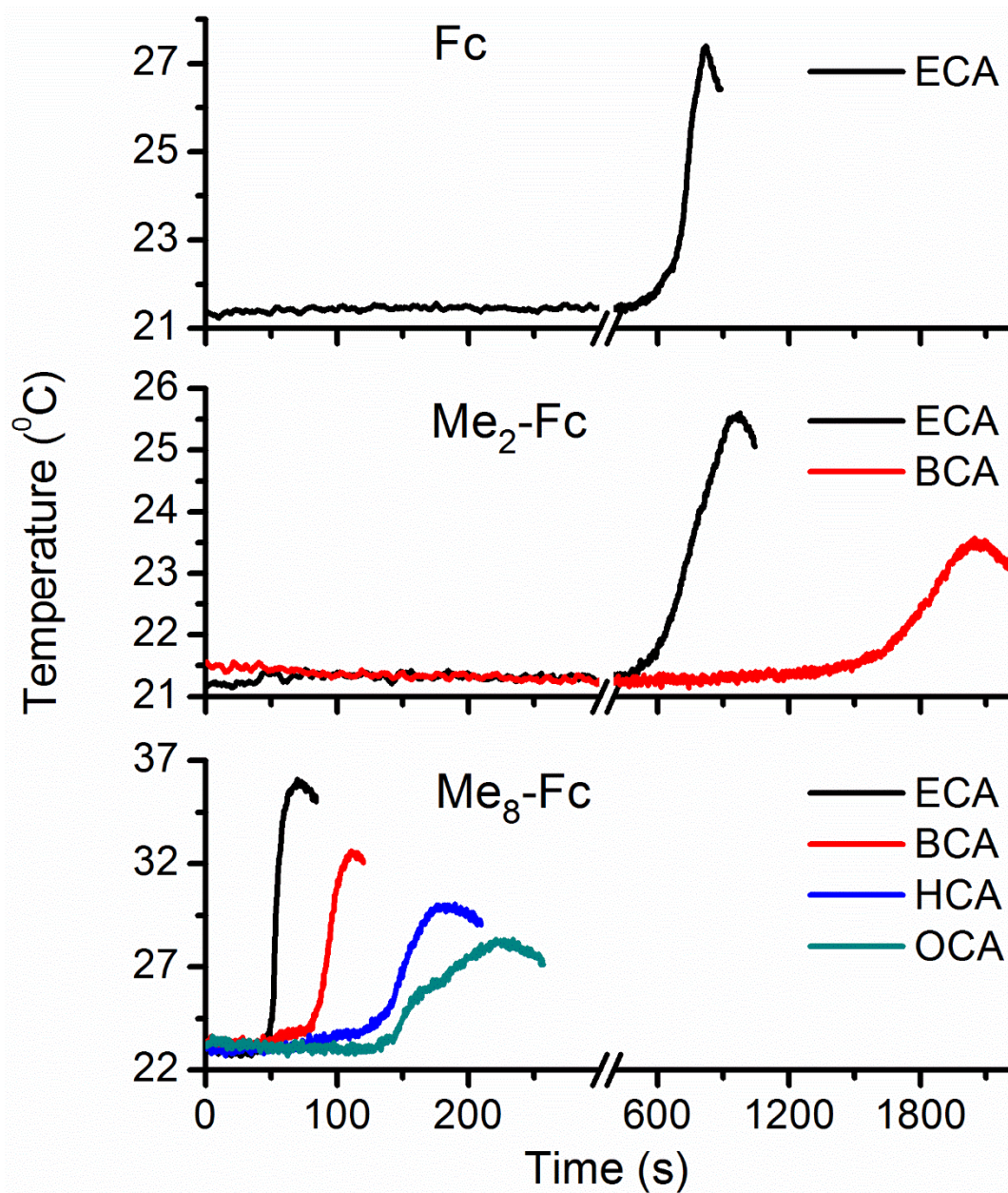


Figure S5. Photopolymerization exotherms measured for: **Fc** and monomer **ECA** ($c_{\text{Fc}} = 2.5 \cdot 10^{-3} \text{ M}$; $\lambda_{\text{exc}} = 405 \text{ nm}$; power = 46 mW cm^{-2}); **Me₂-Fc** and monomers **ECA** and **BCA** ($c_{\text{Me}_2\text{-Fc}} = 0.5 \cdot 10^{-3} \text{ M}$; $\lambda_{\text{exc}} = 405 \text{ nm}$; power = 46 mW cm^{-2}); and **Me₈-Fc** and monomers **ECA**, **BCA**, **HCA** and **OCA** ($c_{\text{Me}_8\text{-Fc}} = 0.5 \cdot 10^{-3} \text{ M}$; $\lambda_{\text{exc}} = 405 \text{ nm}$; power = 46 mW cm^{-2}).

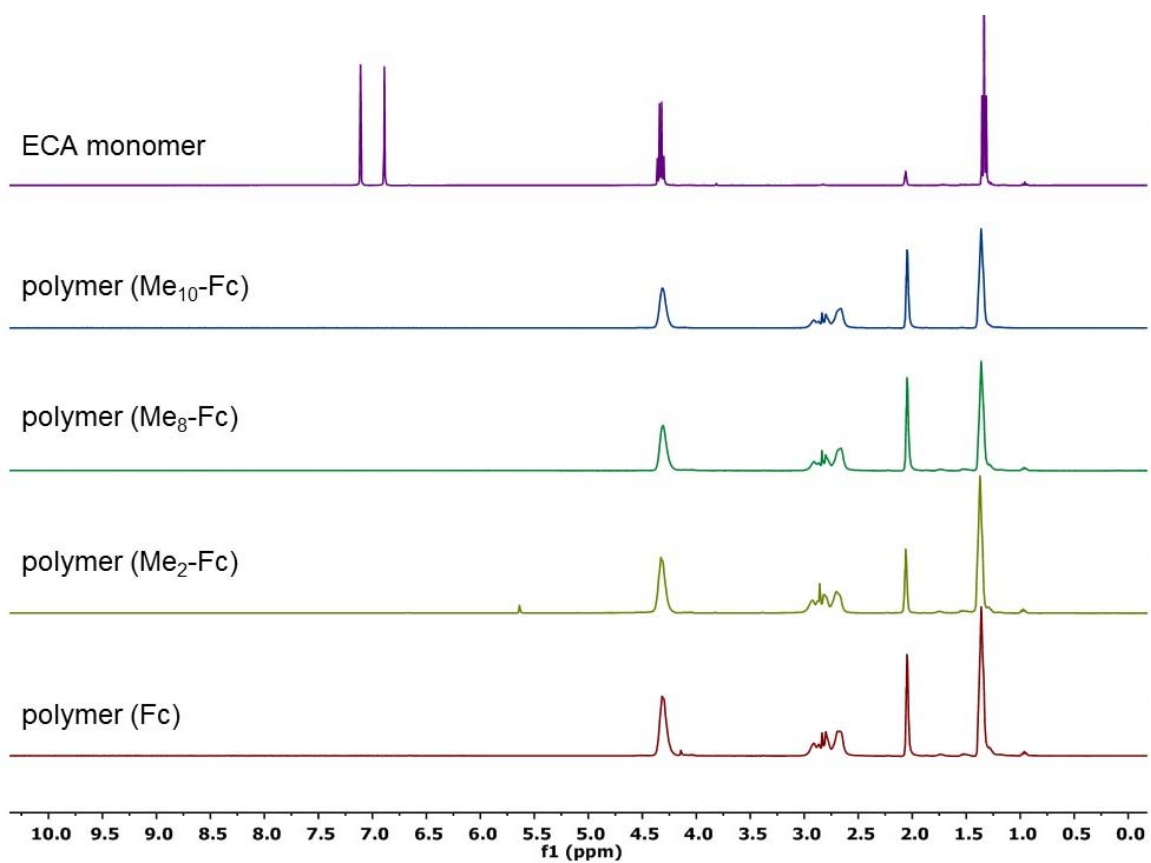


Figure S6. ¹H-NMR spectra (360 MHz, acetone-*d*₆) of ECA in its monomeric form and after photopolymerization with Fc, Me₂-Fc, Me₈-Fc and Me₁₀-Fc.

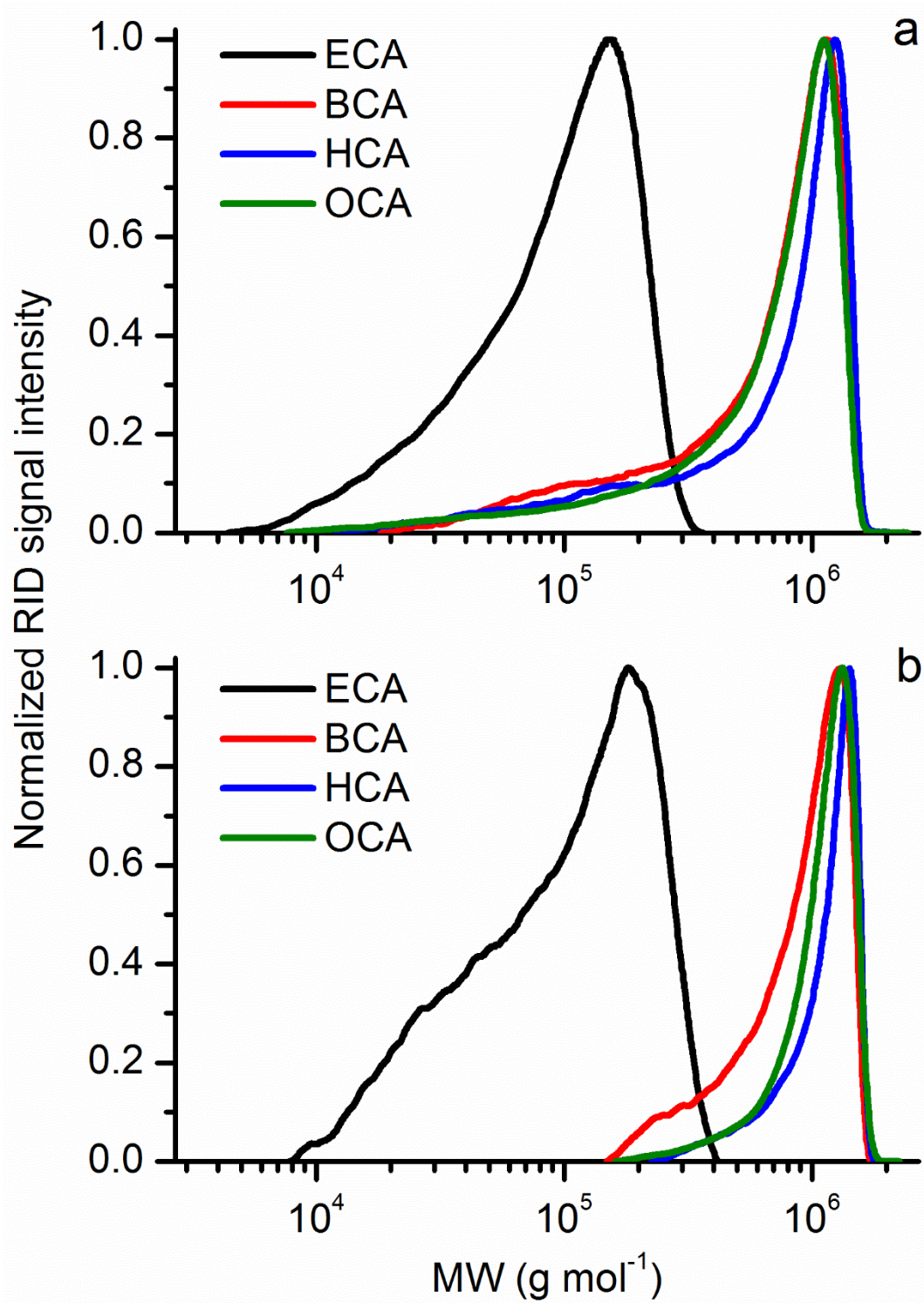


Figure S7. GPC molecular weight distributions for polycyanoacrylates obtained upon either (a) thermal polymerization or (b) photopolymerization with **Me₁₀-Fc** ($c_{\text{Me}_{10}\text{-Fc}} = 0.5 \cdot 10^{-3} \text{ M}$; $\lambda_{\text{exc}} = 405 \text{ nm}$; power = 46 mW cm⁻²).

7. MECHANISM OF PHOTOPOLYMERIZATION

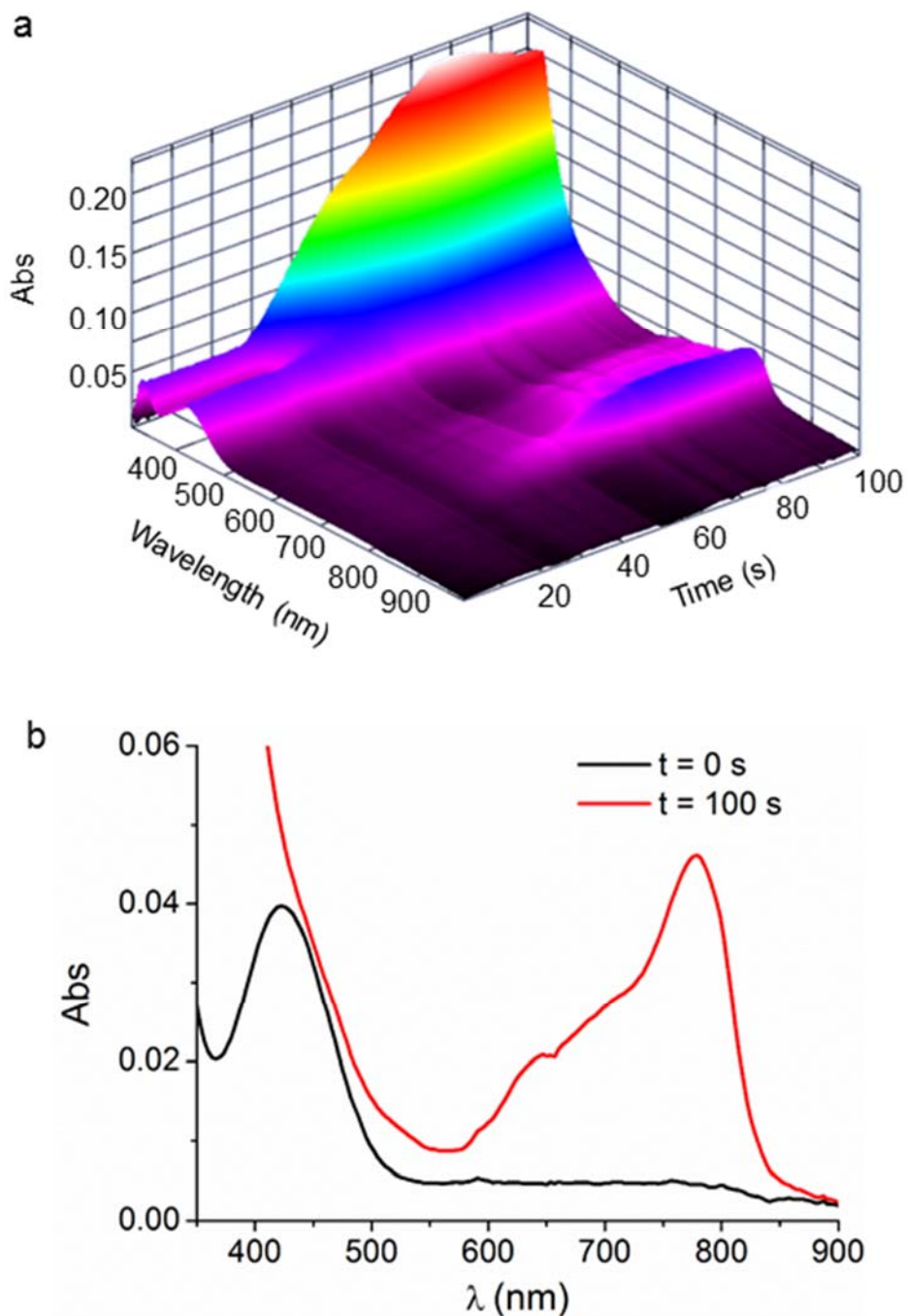


Figure S8. (a) 3D plot representation of the variation of the absorption spectrum of **Me₁₀-Fc** in a 1:1 acetonitrile:toluene mixture (+ 0.1 M *n*-Bu₄NPF₆; $c_{\text{Me}_{10}\text{-Fc}} = 3 \cdot 10^{-3}$ M) upon application of an oxidative potential at $E_{\text{appl}} = +0.35$ V (vs SCE) for 100 s, which should induce the formation of **Me₁₀-Fc⁺**. (b) Absorption spectra registered at $t = 0$ (i.e. for **Me₁₀-Fc**) and 100 s (i.e. for **Me₁₀-Fc⁺**) during this spectroelectrochemical measurement.

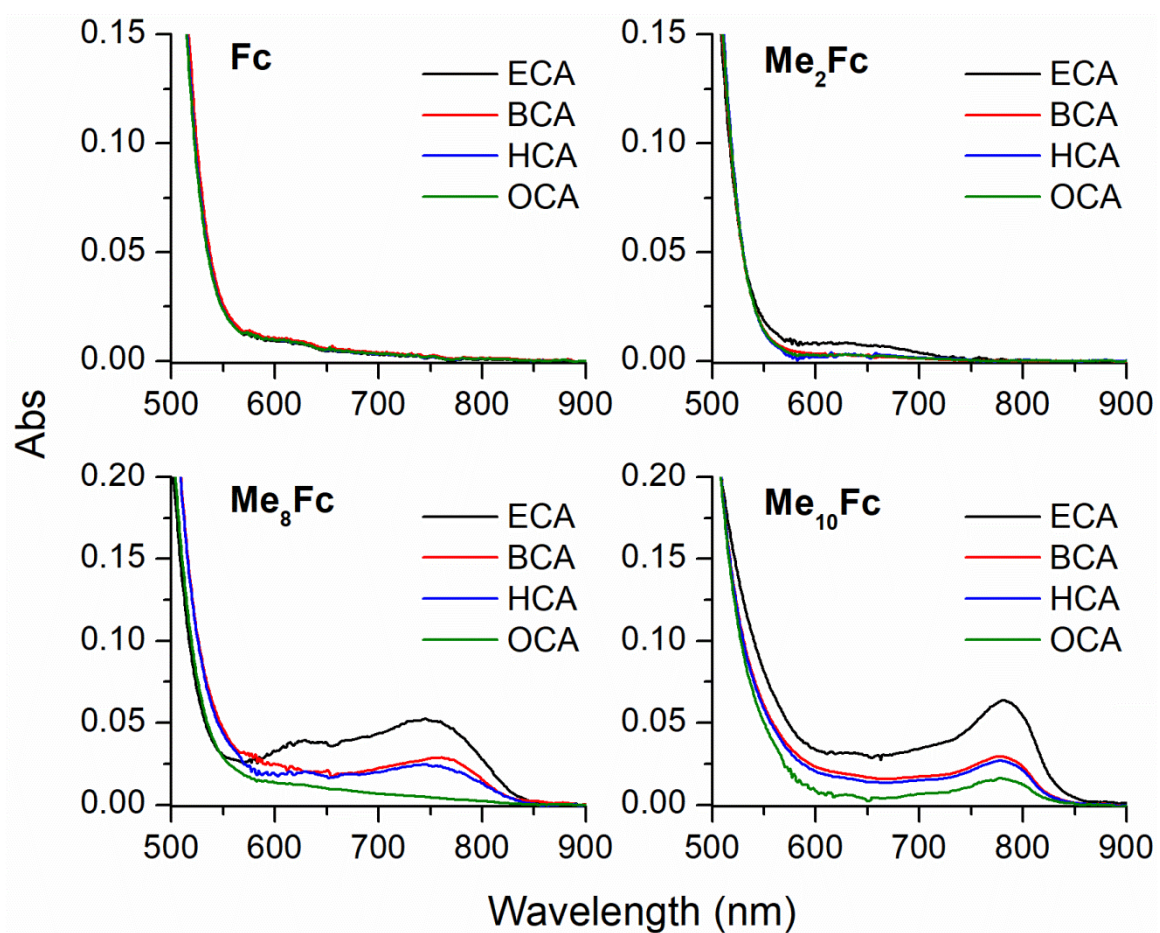


Figure S9. Absorption spectra of concentrated solutions of **ECA**, **BCA**, **HCA** or **OCA** in neat acetonitrile ($c = 1$ M) after addition of different polymethylferrocene derivatives ($c = 7.5 \cdot 10^{-3}$ M).

Table S4. Absorption maxima, association constants^a (K_a) and percentages at photopolymerization conditions^b (%CT) of charge-transfer complexes formed between cyanoacrylate monomers and polymethylferrocenes.

		Me₂-Fc	Me₈-Fc	Me₁₀-Fc
ECA	$\lambda_{\text{abs,max}}$ (nm)	615	745	780
	K_a (M ⁻¹)	0.02 ± 0.01	0.12 ± 0.02	0.16 ± 0.03
	%CT	14	50	57
BCA	$\lambda_{\text{abs,max}}$ (nm)	-	760	777
	K_a (M ⁻¹)	-	0.06 ± 0.01	0.07 ± 0.02
	%CT	-	28	31
HCA	$\lambda_{\text{abs,max}}$ (nm)	-	744	778
	K_a (M ⁻¹)	-	0.05 ± 0.02	0.07 ± 0.01
	%CT	-	21	27
OCA	$\lambda_{\text{abs,max}}$ (nm)	-	-	778
	K_a (M ⁻¹)	-	-	0.04 ± 0.01
	%CT	-	-	18

^a Values determined in acetonitrile solution using the Benesi-Hildebrand method and UV-vis absorption measurements.⁴ ^b Estimated at the photopolymerization conditions reported in Table 2 using the K_a values determined.

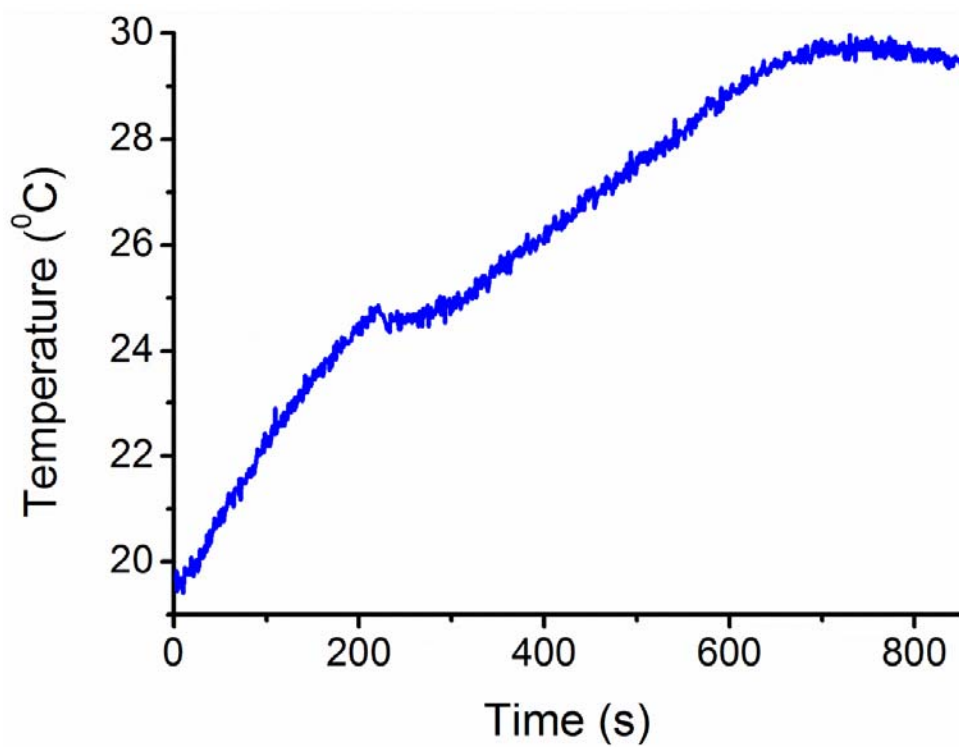


Figure S10. Photopolymerization exotherm measured for **Me₁₀-Fc** and **ECA** ($c_{\text{Me}_{10}\text{-Fc}} = 1.0 \cdot 10^{-3} \text{ M}$; $\lambda_{\text{exc}} = 780 \text{ nm}$; power = 320 mW cm^{-2}).

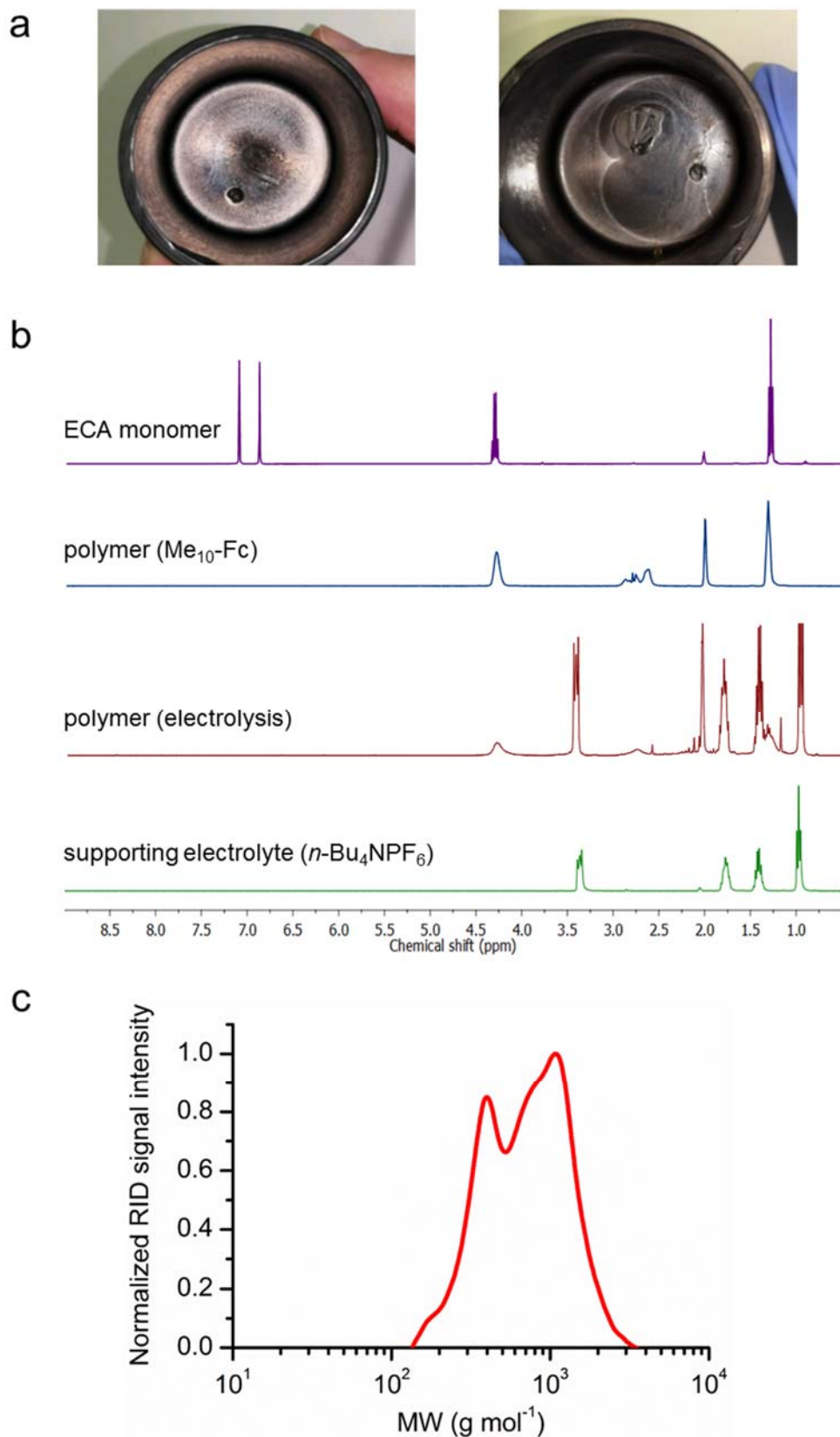


Figure S11. Electropolymerization of ECA in acetonitrile upon application of a reductive potential at $E_{\text{appl}} = -2.1$ V (vs SCE) for 60 min ($c_{\text{ECA}} = 0.04$ M; + 0.1 M n -

Bu₄NPF₆). (a) Photographs of the working electrode before (left) and after (right) of the bulk electrolysis process. The formation of an off-white, thin layer of material onto the surface of the electrode is observed. (b) ¹H NMR spectrum (360 MHz, acetone-*d*₆) of this material (polymer (electrolysis)) which is compared to those registered for ECA, photopolymerized ECA using Me₁₀-Fc, and the supporting electrolyte employed in the electrolysis process. Clearly, signals for both polymerized ECA and *n*-Bu₄NPF₆ are found, which indicates that a layer of polycyanoacrylate was created on the electrode trapping some supporting electrolyte molecules. (c) GPC molecular weight distribution of the polymer material generated by electrolysis.

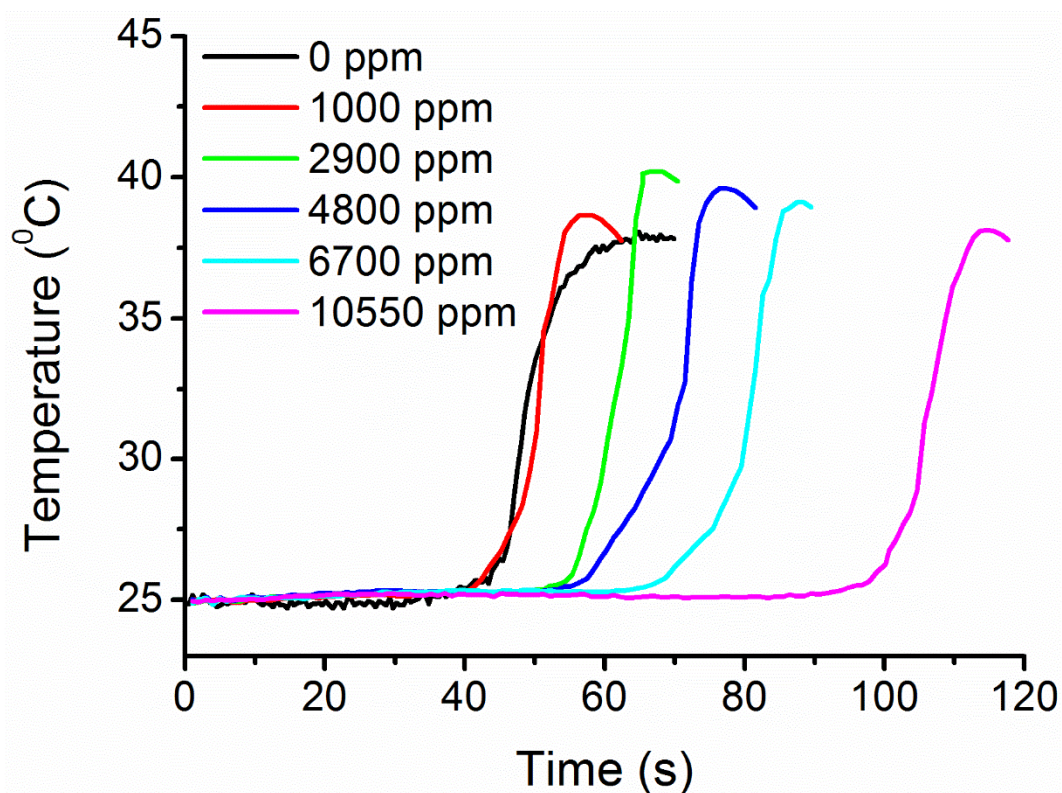
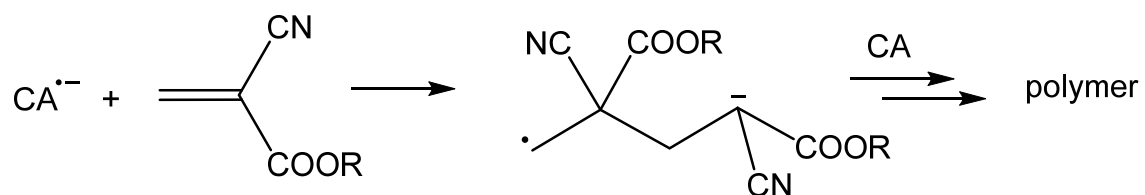
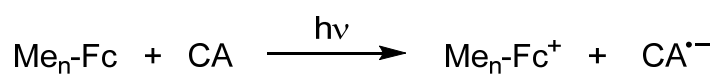


Figure S12. Photopolymerization exotherms of ECA containing $0.5 \cdot 10^{-3}$ M Me₁₀-Fc ($\lambda_{\text{exc}} = 420$ nm, power = 46 mW cm⁻²) and increasing amounts of a radical stabilizer (butylated hydroxyanisole, which was added from a 20000 ppm stock solution in neat ECA).



Scheme S1. Mechanism proposed for the photopolymerization of cyanoacrylates with polymethylated ferrocenes, which initiates through a photoinduced electron transfer process.

8. PHOTOPOLYMERIZATION OF OTHER MONOMERS

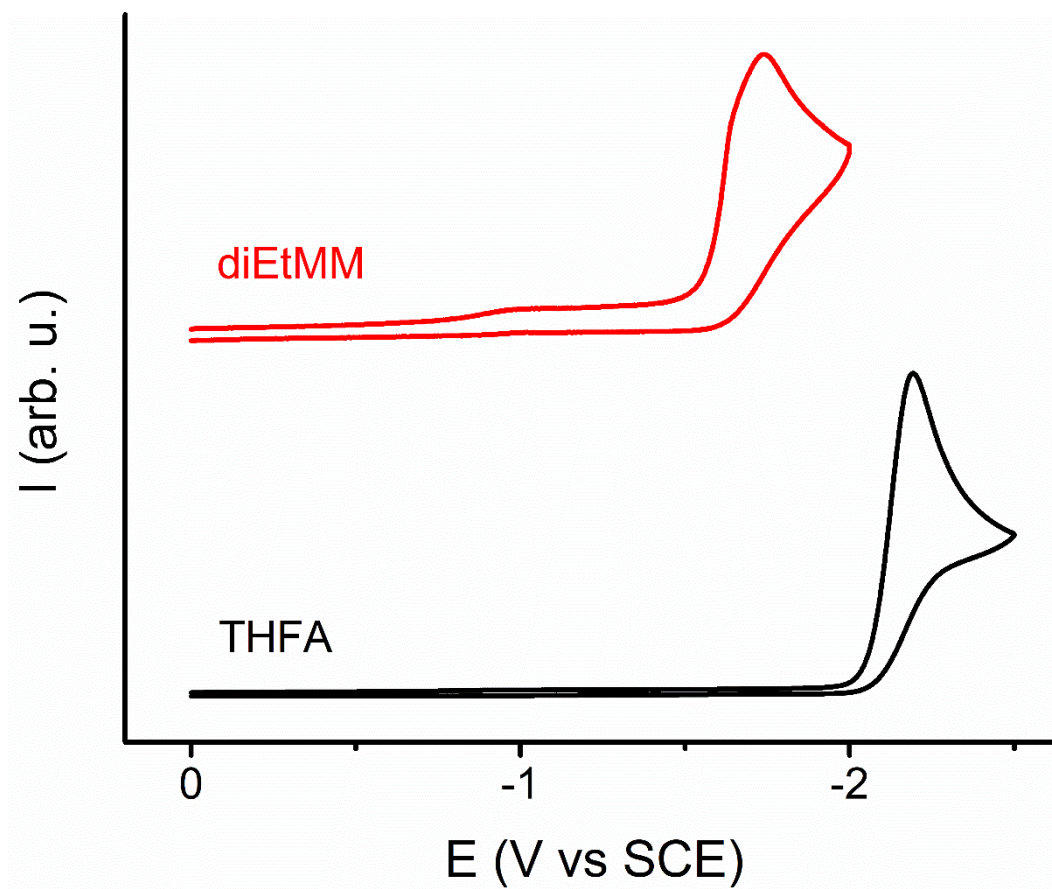


Figure S13. Cyclic voltammograms of **THFA** and **diEtMM** ($c \sim 6 \cdot 10^{-3}$ M) in acetonitrile (+ 0.1 M *n*-Bu₄NPF₆; scan rate 0.5 V s⁻¹).

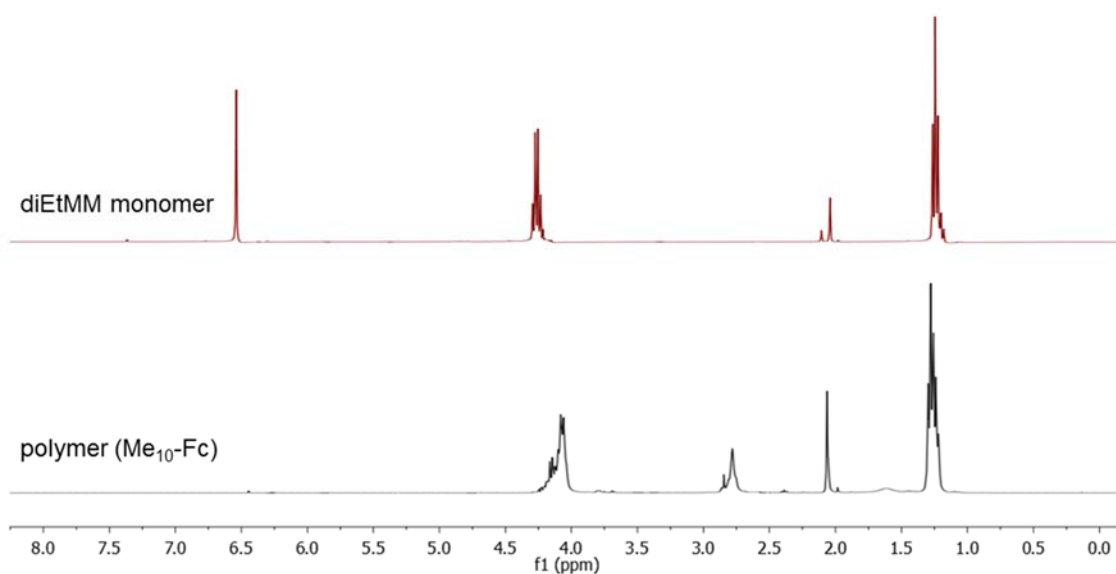


Figure S14. ^1H -NMR spectra (360 MHz, acetone- d_6) of **diEtMM** in its monomeric form and after photopolymerization with **Me₁₀-Fc**.

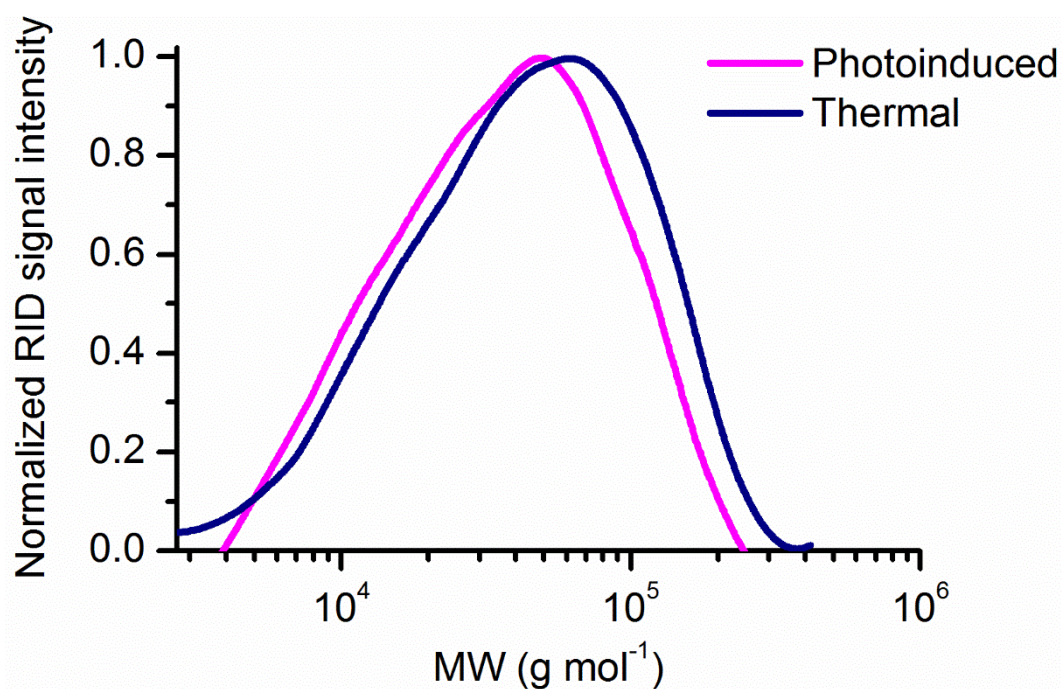


Figure S15. GPC molecular weight distributions for the polymers obtained upon either thermal ($M_n = 3.04 \cdot 10^4 \text{ g mol}^{-1}$; $D = 2.21$) or photoinduced polymerization of **diEtMM** with **Me₁₀-Fc** ($c_{\text{Me}_{10}\text{-Fc}} = 30 \cdot 10^{-3} \text{ M}$; $\lambda_{\text{exc}} = 405 \text{ nm}$; power = 46 mW cm^{-2} ; $M_n = 2.76 \cdot 10^4 \text{ g mol}^{-1}$; $D = 1.96$).

9. REFERENCES

- (1) Kalenda, P.; Veselý, D.; Kalendová, A.; Št'áva, V. Ferrocene-Based Catalyst Systems for Alkyd Paint Drying. *Pigm. Resin Technol.* **2010**, *39*, 342-347.
- (2) Cooke, B. D.; Allen, K. W. Cyanoacrylates and their Acid Values, *Int. J. Adhesion Adhesives* **13**, **1993**, 73-76.
- (3) Berberich, M.; Krause, A.; Orlandi, M.; Scandola, F.; Würthner, F. Toward Fluorescent Memories with Nondestructive Readout: Photoswitching of Fluorescence by Intramolecular Electron Transfer in a Diarylethene-Perylene Bisimide Photochromic System. *Angew. Chem. Int. Ed.* **2008**, *47*, 6616-6619.
- (4) Frey, J. E.; Du Pont, L. E.; Puckett, J. J. Formation Constants of Radical-Ion Pairs and Charge-Transfer Complexes of Tetracyanoethylene with Group 8 Metallocenes. *J. Org. Chem.* **1994**, *59*, 5386-5392.